TUM School of Natural Science
Department of Physics
Technical University of Munich

A Stochastic Tensor Network Approach for Non-Markovian Dissipative Dynamics of Quantum Impurity Models

Madhav Menon

Thesis for the attainment of the academic degree

Bachelor of Science (B.Sc.)

at the Department of Physics of the Technical University of Munich.

Examiner:
Prof. Dr. Frank Pollmann

Supervisor:
Prof. Dr. Frank Pollmann

Submitted:
Munich, 06.08.2024

I hereby declare that this thesis is entirely the result of my own work except where otherwise indicated. I have only used the resources given in the list of references.

Munich, 06.08.2024 Madhav Menon

Abstract

This thesis explores the numerical simulation of quantum impurity models using non-markovian stochastic tensor network methods. This thesis uses a novel approach called Hierarchy of Matrix Product States (HOMPS) to simulate bosonic quantum impurity models exactly. My supervisors and I introduce the Hierarchy of Grassmannian Tensor Product States (HOGTPS) to simulate fermionic impurity models. The main result of this thesis is to propose this method to simulate fermionic and hybrid open quantum systems. Implementing and benchmarking HOGTPS is not shown in this thesis, however, it will be the next step in this journey.

I discuss in detail several key theoretical fundamentals required to understand the tensor network approaches and the quantum impurity models. For the impurity models explored, I focus on the spin-boson model and fermionic impurity models such as the Kondo model and the Simple Impurity Anderson Model. I take a step further and explore experimental realizations of spin-boson models through engineered setups from ultra-cold atoms and Josephson junctions and discuss these engineered Hamiltonians to explore the field of quantum simulation. Numerical results are only gained for the spin-boson model and its experimental realizations.

Contents

1 Introduction

Strongly correlated systems exhibited in quantum impurity models are a rich area of theoretical physics where abundant theoretical development is still at the forefront of the field. A better understanding or testing of proposed theories requires deriving numerical or analytical solutions, which are a big challenge. Tensor networks are a powerful tool enabling the numerical analysis for these models [1]. From the success of the Density Matrix Renormalization group (DMRG) in the early 90s, employing the tensor network ansatz to simulate the evolution of a quantum system for one dimension has been very practical [1].

Although over 30 years of fascinating development have followed since DMRG, several different numerical algorithms have been developed to obtain numerical results for different models in condensed matter and high-energy physics. One of these methods developed by D.Seuess is known as the Hierarchy of Pure states [2] which develops upon the Non-Markovian Quantum State Diffusion by giving an exact solution for the dynamics of an open quantum system. An extension of this was developed by [3] to form a Matrix Product State (MPS) ansatz known as the Hierarchy of Matrix Product States, which gives efficient simulations for a quantum system coupled to a bosonic bath in 1D [3].

There are several open problems remaining within this method that have yet to be addressed. Within the context of impurity problems, the exact simulation of the dynamics of a quantum system coupled to a fermionic bath in 1-D is an example, mainly due to the anticommuting behaviour of the bath, also the simulation of the noise process accompanying fermionic HOPS is very inefficient to simulate [2].

The main result of this thesis is addressing this problem by implementing a new tensor network method called the Hierarchy of Grassmannian Tensor Product States (HOGTPS) to simulate quantum systems coupled to a fermionic bath. I will first explore the formalism behind HOPS and the Fermionic HOPS by first discussing the fermionic coherent state representation. Then I will discuss tensor networks and one algorithm used for Hamiltonian evolution known as the Time Dependent Variational Principle (TDVP). Afterwards, the formalism behind the main tensor network approach implemented for the spin-boson model known as HOMPS will be discussed before introducing the tensor network method developed from this thesis called HOGTPS. After a theoretical introduction, numerical results are shown for the spin-boson models using HOMPS, whilst HOGTPS ansatz is proposed for fermionic impurity models.

2 Fermion Coherent States

There exist different representations for states within a Hilbert space, such as the Fock-Bargmann representation leading to the second quantization formalism. The Gaussian coherent state representation of basis states is a powerful tool for evaluating the path integral for theories which are not only based on canonical quantization (such as fermions). Similar steps to derive a coherent state representation for bosons cannot be followed for the case of fermions due to the anti-commuting relations. This motivates the implementation of a new kind of nilpotent and symmetric algebra known as the Grassmann algebra. [4]. Nilpotence directly encodes the Pauli exclusion principle, allowing for a mathematical structure to describe the physical property of fermions. An irreducible representation of the rotation group $SO(2n, \mathbb{R})$ for a system of n fermions called the spin representation is also a mathematically equivalent approach [4], avoiding the use of Grassmann algebra. However, in the context of this thesis, the Grassmann representation is imperative towards successfully simulating a fermionic bath [2], hence motivating this section to introduce the relevant formalism.

Considering a Hilbert space spanned by a set of harmonic oscillators $|n\rangle$ and [$\hat{a}^\dagger$, $\hat{a}$] be the standard creation and annihilation operators that satisfy standard commutation relation (CCR), these operators generate harmonic oscillator states, which is well known, in terms of the vacuum state $|0\rangle$ by :

$$|n\rangle = \frac{1}{\sqrt{n!}}(\hat{a}^\dagger)|0\rangle \tag{2.1}$$

A coherent state $|z\rangle$ is given by:

$$|z\rangle = e^{z\hat{a}^\dagger}|0\rangle, \quad \langle z| = \langle 0|e^{\bar{z}\hat{a}} \tag{2.2}$$

Where z is an arbitrary complex number with $\bar{z}$ being its complex conjugate. This coherent state representation in equation (2.2) is relevant for bosons. The relevant expression for fermions will be explained in the next section.

2.1 Grassmann Algebra

A Grassmann algebra $\mathbb{A}$ on $\mathbb{R}$ or $\mathbb{C}$ is an associative algebra generated by a unit and a set of generators $\{\theta_i\}$ that satisfy the anti-commutation relations:

$$\theta_i\theta_j + \theta_j\theta_i = 0 \quad \forall i, j \tag{2.3}$$

If the number of generators n is finite, the elements of the algebra form a vector space of finite dimension 2^n over $\mathbb{R}$ or $\mathbb{C}$. All elements can be written as linear combinations of the elements $A_v, v = 1, \ldots, 2^n$:

$$A_\nu \in \{1 \text{ and } \{\theta_{i_1}\theta_{i_2}\ldots\theta_{i_p}\} \text{ with } i_1 < i_2 < \cdots < i_p, 1 \leq p \leq n\}. \tag{2.4}$$

A is a graded algebra, this means that for each monomial $\theta_{i_1}\theta_{i_2}\theta_{i_3}\ldots\theta_{i_p}$, one can associate an integer p that counts the number of generators in a product. Furthermore, if A_p and A_q are two monomials of degree p and q respectively, then the swapping between the two monomials is:

$$A_pA_q = (-1)^{pq}A_qA_p \tag{2.5}$$

Another important property of the algebra relevant to defining the fermionic coherent states is that all elements in a Grassmann algebra, considered as functions of a generator θ_i are first-degree polynomials

(affine functions).

Differentiating Grassmann algebras can be derived easily by considering the Nilpotent property [5].

$$\begin{array}{l} A = A_1 + \theta_i A_2 \\ \frac{\partial A}{\partial \theta_i} = A_2 \end{array} \tag{2.6}$$

The inherent nilpotent property of Grassmann algebras results in the operator $\frac{\partial}{\partial \theta_i}$ to be nilpotent. Left and right derivatives can also be defined in such a way that a left/right derivative consists of acting the operator $\frac{\partial}{\partial \theta_i}$ commuting θ_i to the left/right in all monomials before suppressing it.

Similar considerations are done when taking an integral of Grassmann variables, defined by:

$$\int \mathrm{d}_i A \equiv \frac{\partial}{\partial \theta_i} A, \quad \forall A \in \mathbb{A} \tag{2.7}$$

Considering more relevant situations, where integrations of algebras with the double family of generators $\{\theta_i, \bar{\theta}_i\}, i = 1, \ldots, n$ related by the complex conjugation, the integration is considered of the form:

$$I = \int \mathrm{d}\theta \mathrm{d}\bar{\theta} f(\theta, \bar{\theta}) \tag{2.8}$$

General integration rules can then be formulated as:

$$\begin{array}{lll} \int d\xi 1 = 0 & \leftrightarrow & \partial_\xi 1 = 0 \\ \int d\xi \xi = 1 & \leftrightarrow & \partial_\xi \xi = 1 \end{array} \tag{2.9}$$

Where the pair $(\theta, \bar{\theta})$ represents any pair of conjugate generators. By considering these rules to a general analytical function $A(\bar{\xi}, \xi)$, the rules are:

$$\begin{aligned} \int d\xi A(\bar{\xi}, \xi) &= \int d\xi \left(a_0 + a_1 \xi + \bar{a}_1 \bar{\xi} + a_{12} \bar{\xi} \xi \right) = a_1 - a_{12} \bar{\xi} \\ \int d\bar{\xi} A(\bar{\xi}, \xi) &= \int d\xi \left(a_0 + a_1 \xi + \bar{a}_1 \bar{\xi} + a_{12} \bar{\xi} \xi \right) = \bar{a}_1 + a_{12} \xi \\ \int d\bar{\xi} d\xi A(\bar{\xi}, \xi) &= - \int d\xi d\bar{\xi} A(\bar{\xi}, \xi) = -a_{12} \end{aligned} \tag{2.10}$$

From these considerations, the delta function can be straightforwardly shown as:

$$\delta(\bar{\xi}, \xi) = \int \mathrm{d}\eta e^{-\eta(\xi - \bar{\xi})} \tag{2.11}$$

Where $\xi, \bar{\xi}$ and η are Grassmann variables.

The final important consideration of Grassmann algebras that are very relevant for determining the Grassmann tensor network approach is the Grassmann Gaussian integrals. These Gaussian integrals are defined with an integration over two families of generators $\{\theta_i, \bar{\theta}_i\}$. By considering the integral:

$$\mathcal{Z}(\mathbf{K}) = \int \mathrm{d}\theta_1 \mathrm{d}\bar{\theta}_1 \mathrm{d}\theta_2 \mathrm{d}\bar{\theta}_2 \ldots \mathrm{d}\theta_n \mathrm{d}\bar{\theta}_n \exp\left(\sum_{i,j=1}^{n} \bar{\theta}_i K_{ij} \theta_j \right). \tag{2.12}$$

This integral can be simplified by using the rules of the Grassmann integral. Focusing on the integrated, the argument of the exponential function contains only terms belonging to $\mathbb{A}^+$, which commute. With this information, the integrand can be written as:

$$\begin{aligned} \exp\Big(\sum_{i,j=1}^{n} \bar{\theta}_i K_{ij} \theta_j \Big) &= \prod_{i=1}^{n} \exp\Big(\bar{\theta}_i \sum_{j=1}^{n} K_{ij} \theta_j \Big) \\ &= \prod_{i=1}^{n} \left(1 + \bar{\theta}_i \sum_{j_i=1}^{n} K_{ij_i} \theta_{j_i} \right). \end{aligned} \tag{2.13}$$

This leads to a Gaussian integral over Grassmann variables by also introducing another copy of the Grassmann algebra $\mathbb{A}$ whose generators are denoted by $\{\zeta_i, \bar{\zeta}_i\}$ of the form :

$$\mathcal{Z}[K] = \int \left(\prod_{i=1}^{N} d\bar{\theta}_i d\theta_i \right) e^{-\sum_{i,j} \bar{\xi}_i K_{ij} \theta_j + \bar{\theta}_i \zeta_i + \bar{\zeta}_i \xi_i} \tag{2.14}$$

The above expression gives a more general expression for performing Gaussian integrals over Grassmann algebras. This defines the backbone for performing basic operations with Grassmann algebras, which is required to understand Grassmann tensor networks. However, the notion of "creating" or "annihilating" a Grassmann algebra is not defined. To address this, the Grassmann representation of fermionic Fock spaces is introduced and the generalized Grassmann algebra is mentioned to introduce the notion of ladder operators with Grassmann variables.

2.2 Grassmann Generalization from Weyl-Heisenberg Algebra

To understand the notion of ladder operators in terms of Grassmann generators, a generalized definition of Grassmann algebra needs to be defined from a Weyl-Heisenberg algebra [6]. An introduction to Weyl-Algebra can be found in [4]. A Qudit algebra used in [6] is represented by generalized Grassmann variables, which is the main result of this paper. However, this result can not be used within this thesis as the Qudit algebra does not satisfy fermionic commutation relations, although, the methodology in deriving such a representation in [6] can be used to intuitively understand how one could perform raising and lowering operations on a Grassmann algebra.

2.2.1 Generalized Grassmann Variables

From the properties of Grassmann algebra discussed in the previous sections, a general expression can be achieved from the polynomial expansion for symmetric Grassmanian generators θ. A generalized Grassmann variable can be defined as:

$$\eta = \sum_{i=1}^{k} \theta_i \quad \eta = \sum_{i=1}^{k} \bar{\theta}_i \tag{2.15}$$

By definition, these Grassmann variables are Nilpotent (as the square of the variable is zero). $\bar{\theta}$ is the conjugate of θ. From [6], A symmetric θ-polynomial can be defined as :

$$e_n(\vec{\theta}) = \sum_{i_1 < i_2 < \cdots < i_n} \theta_{i_1} \theta_{i_2} \cdots \theta_{i_n}, \quad \text{for} \quad n = 1, 2, \cdots, k \quad \text{and} \quad e_0(\vec{\theta}) = 1 \tag{2.16}$$

Where the vector containing the generators $\vec{\theta} = (\theta_1, \theta_2, \cdots, \theta_n)$. From (2.16), the $n - th$ power of the Grassmann variable η (2.15) can be expressed in terms of symmetric θ polynomials as:

$$\eta^n = n! e_n(\vec{\theta}) \quad \text{for} \quad n = 1, 2, \cdots, k \tag{2.17}$$

The nilpotency condition of a Grassmann variable requires the $k+1$-th exponent of the generalized Grassmann variable (2.17) to be zero. The η-derivative can be derived in an analogous procedure. By first defining a differential-$\frac{\partial}{\partial\theta}$ and $\frac{\partial}{\partial\bar{\theta}}$ operator as:

$$\frac{\partial}{\partial \eta} = \sum_{i=1}^{k} \frac{\partial}{\partial \theta_i}, \qquad \frac{\partial}{\partial \bar{\eta}} = \sum_{i=1}^{k} \frac{\partial}{\partial \bar{\theta}_i}. \tag{2.18}$$

Using properties in equation (2.9), a generalized differential-$\frac{\partial}{\partial\theta}$ operator is defined as:

$$g_n = \sum_{i_1 < i_2 < \cdots < i_n} \partial_{\theta_{i_1}} \partial_{\theta_{i_2}} \cdots \partial_{\theta_{i_n}}, \quad \text{for} \quad n = 1, 2, \cdots, k \quad \text{and} \quad g_0 = 1. \tag{2.19}$$

From [6], the raising and lowering of a symmetric analytic function can be gained by acting the generalized Grassmann variable and generalising Grassmann derivative respectively:

$$\eta e_n(\vec{\theta}) = e_{n+1}(\vec{\theta}), \quad \frac{\partial e_n(\vec{\theta})}{\partial \eta} = e_{n-1}(\vec{\theta}) \tag{2.20}$$

This result is similar to the annihilation and creation operators for a generalized Weyl-Heisenberg algebra. The main difference is the normalization factors and the algebra commutation rules. The notion of a generalized Grassmann algebra is useful when discussing Grassmann tensor product states [7], where the basis of the tensors is described in terms of Grassmann generators. In [8], the authors use a different mapping compared to equation (2.20), where essentially the fermionic creation/annihilation operator is mapped to a Grassmann generator/conjugate generator.

2.3 Fermionic Fock Spaces and Grassmann Representation

For N fermions, the Hilbert space is spanned by the anti-symmetrized states $|n_1, \ldots, n_N\rangle$. A general state in this Hilbert space is then given by :

$$n_1, \ldots, n_N\rangle = (c_1^\dagger)^{n_1} \ldots (c_N^\dagger)^{n_N}|0\rangle \tag{2.21}$$

Projecting this state onto the wave function $\langle n_1, \ldots, n_N|\Psi$ is fully antisymmetric.

Let $\bar{\xi}_i, \xi_i$, with $i = 1, \ldots, N$ be a set of $2N$ Grassmann variables, which are the generators of the Grassmann algebra. By definition, Grassmann variables satisfy the following properties:

$$\{\xi_i, \xi_j\} = \{\bar{\xi}_i, \bar{\xi}_j\} = \{\xi_i, \bar{\xi}_j\} = \xi^2 = \bar{\xi}^2 = 0 \tag{2.22}$$

From the above property, Grassmann variables behave as a set of time-ordered fermion operators. These variables must also anti-commute with fermion operators:

$$\{\xi_i, c_j\} = \{\bar{\xi}_i, c_j^\dagger\} = \{c_j, \bar{\xi}_j\} = \{c_j^\dagger, \bar{\xi}_j\} = 0 \tag{2.23}$$

These properties allow for the definition of coherent states to be:

$$\begin{aligned} |\xi\rangle &\equiv e^{-\xi c^\dagger}|0\rangle \\ \langle\xi| &\equiv \langle 0|e^{\bar{\xi}c} \end{aligned} \tag{2.24}$$

We can Taylor expand the exponential term with the Grassmann variable to the second term because the exponentials of Grassmann variables are zero (Nilpotency).

$$e^{-\xi c^\dagger} = 1 - \xi c^\dagger \tag{2.25}$$

Taking the inner product of two fermionic coherent state $|\xi\rangle$ and $|\psi\rangle$ is given by:

$$\langle\xi|\psi\rangle = \langle 0|e^{\bar{\xi}c - \psi c^\dagger}0\rangle = 1 + \bar{\xi}\psi = e^{\bar{\xi}\psi} \tag{2.26}$$

Since the commutator $[\xi_i c_i^\dagger, \xi_j c_j^\dagger]$ vanishes, this gives clean expressions when considering the N fermion coherent state representation:

$$|\xi\rangle = |\xi_1, \ldots, \xi_N\rangle = \Pi_{i=1}^N e^{-\xi_i c_i^\dagger}|0\rangle \equiv e^{\sum_{i=1}^N \xi_i c_i^\dagger}|0\rangle \tag{2.27}$$

By using the above definition for fermionic coherent states and the rules for Grassmann algebras mentioned in the previous section, the properties for these coherent states can now be mentioned. These coherent states can be written can be expressed as:

$$|\{\xi_j\}\rangle = e^{-\sum_j \xi_j c_j^\dagger}|0\rangle, \quad \langle\{\xi_j\}| = \langle 0|\, e^{\sum_j \bar{\xi}_j c_j} \tag{2.28}$$

With relations with fermionic annihilation and creation operators as:

$$c_i|\{\xi_j\}\rangle = \xi_i|\{\xi_j\}\rangle \quad c_i^\dagger|\{\xi_j\}\rangle = -\partial_{\xi_i}|\{\xi_j\}\rangle \quad \langle\{\xi_j\}|c_i = \partial_{\bar{\xi}_i}\langle\{\xi_j\} \quad |\langle\{\xi_j\}|c_i^\dagger = \bar{\xi}_i\langle\{\xi_j\}| \tag{2.29}$$

The inner product between two coherent states is given by:

$$\langle\{\xi_j\}|\{\xi_j'\}\rangle = e^{\sum_j \bar{\xi}_j\xi_j} \tag{2.30}$$

Similarly, the Resolution of the Identity operator of a single Grassmann variable is given by:

$$I = \int (\Pi_{i=1}^N \mathrm{d}\bar{\xi}_i \mathrm{d}\xi_i) e^{-\sum_{i=1}^N \bar{\xi}_i\xi_i} |\{\xi_i\}\rangle\langle\{\xi_i\}| \tag{2.31}$$

To express a generic state $|\Psi\rangle$ in terms of the resolution identity (2.31), For $\Psi(\bar{\xi}) = \Psi(\bar{\xi_1}, \ldots, \bar{\xi_N})$. This state can be expanded in fermion coherent states as:

$$|\Psi\rangle = \int (\Pi_{i=1}^N \mathrm{d}\bar{\xi} \mathrm{d}\xi) e^{-\sum_{i=1}^N \bar{\xi}_i\xi_i} |\Psi(\xi)\rangle\langle\{\xi_i\}| \tag{2.32}$$

With this state, the corresponding matrix elements can be expressed as:

$$\langle\xi|c_j|\xi\rangle = \partial_{\bar{\xi}_j}\Psi(\bar{\xi}), \quad \langle\xi|c_j^\dagger|\Psi\rangle = \bar{\xi_j}\Psi(\hat{}) \tag{2.33}$$

Calculating expectation values for normally ordered operators $A(\{c_j^\dagger\}, \{c_j\})$, let $|0\rangle$ define an empty state. This is not interchangeable with a vacuum state since it is not in the sector of the ground state of systems of interest [5]. The matrix elements of this ordered operator in the coherent states $|\xi_i\rangle$, $|\bar{\xi}\rangle$ can be shown as:

$$\langle\xi|A(\{c_j^\dagger\}, \{c_j\})|\bar{\xi}\rangle = e^{\sum_i \bar{\xi}_i\xi_i'} A(\{\bar{\xi_k}\}, \xi_j') \tag{2.34}$$

If considering the fermion number operator $\hat{N}$, the expectation value of this operator in the coherent state will be:

$$\frac{\langle\xi|\hat{N}|\xi\rangle}{\langle\xi|\xi\rangle} = \sum_j \bar{\xi_j}\xi_j \tag{2.35}$$

3 Non-Markovian Quantum State Diffusion and Hierarchy of Pure states

The main result of evolving the wave function using NMQSD is that it successfully expresses the reduced density matrix as an ensemble average over stochastic pure states.

The reduced density matrix shown in $(8.4$)is first modified to represent Bargmann coherent states [9] $|z_\lambda\rangle := e^{z_\lambda a_\lambda^\dagger}|0\rangle_\lambda$ with coherent states $z_\lambda \in \mathbb{C}$ and $|0\rangle_\lambda$ representing the ground state of the respective mode with index λ. This gives a new expression for the reduced density matrix:

$$\rho_{\text{sys}}(t) = \text{Tr}_{\text{env}}(|\Psi(t)\rangle\langle\Psi(t)|) = \int \text{d}^2\mathbf{z} \frac{e^{-|\mathbf{z}|^2}}{\pi^{N_B}} \langle\mathbf{z}|\Psi(t)\rangle\langle\Psi(t)|\mathbf{z}\rangle \tag{3.1}$$

The integral is over a complex vector space with elements $\mathbf{z} := (z_1, \dots z_{N_B})^T$. Working with the interaction picture to the environmental Hamiltonian is advantageous as it eliminates the oscillator dynamics of the system. This does not affect the system as the propagator in the interaction picture only acts on the environment. This gives the Schrödinger equation for the wave function as:

$$\text{i}\partial_t|\Psi(t)\rangle = U_{\text{env}}^\dagger(t)(H - H_{\text{env}})U_{\text{env}}(t)|\Psi(t)\rangle = \left(H_{\text{sys}} + \sum_\lambda g_\lambda^* e^{\text{i}\omega_\lambda t} L a_\lambda^\dagger + g_\lambda e^{-\text{i}\omega_\lambda t} L^\dagger a_\lambda\right)|\Psi(t)\rangle \tag{3.2}$$

The coherent state labels in the equation (3.1) can be interpreted stochastically as complex-valued Gaussian distributed random variables with zero mean and covariances. This introduces more constraints to the problem [2]:

$$\mathcal{M}(z_\lambda z_{\lambda'}) = \mathcal{M}(z_\lambda^* z_{\lambda'}^*) = 0 \quad \text{and} \quad \mathcal{M}(z_\lambda z_{\lambda'}^*) = \delta_{\lambda,\lambda'} \, .$$

Over the coherent state labels:

$$\rho_{\text{sys}}(t) = \mathcal{M}_{\mathbf{z}}\left(|\psi(\mathbf{z}^*, t)\rangle\langle\psi(\mathbf{z}, t)|\right)$$

The stochastic pure state is then expressed as:

$$|\psi(\mathbf{z}^*, t)\rangle := \langle\mathbf{z}|\Psi(t)\rangle \, .$$

For numerical stabilities, a non-linear expression of the expectation value may be considered. This is allowed since a property of the Bargmann coherent states is that $\langle\Psi(t)|z\rangle$ is holomorphic in z and thus does not depend on z^*.

The results can be summarized into the dynamics of the reduced state if the dynamics of the stochastic pure state are known. Using $\langle\mathbf{z}|a_\lambda|\Psi\rangle = \partial_{z_\lambda^*}\langle\mathbf{z}|\Psi\rangle$ and $\langle\mathbf{z}|a_\lambda^\dagger|\Psi\rangle = z_\lambda^*\langle\mathbf{z}|\Psi\rangle$,The Schrödinger equation in (3.2) can be expressed as:

$$\partial_t\psi(\mathbf{z}^*, t) = \left[-\text{i}H_{\text{sys}} + z^*(\mathbf{z}^*, t)L - \text{i}L^\dagger \sum_\lambda g_\lambda e^{-\text{i}\omega_\lambda t}\partial_{z_\lambda^*}\right]\psi(\mathbf{z}^*, t) \tag{3.3}$$

Where $z^*(\mathbf{z}^*, t) := -\text{i}\sum g_\lambda^* z_\lambda^* e^{\text{i}\omega_\lambda t}$ is the complex Gaussian stochastic noise process.

An important step in the derivation is that although the stochastic pure state is an element of the system Hilbert space, the number of bath modes is still present in the equation (3.3) due to expressing the

states in Bargmann coherent states. Taking the limit $\Delta t \to 0$ leads to the differential form of the NMQSD equation [10]:

$$\partial_t \psi_t[\eta^*] = \left[-\mathrm{i}H_{\mathrm{sys}} + \eta^*(t)L - L^\dagger \int_0^t \mathrm{d}s\, \alpha(t-s)\frac{\delta}{\delta\eta^*(s)}\right]\psi_t[\eta^*] \tag{3.4}$$

This results in NMQSD being a functional stochastic process. The local nature of the equation for the stochastic pure state (3.4) is not problematic as it contains a convolutional-like integral which probes how the stochastic pure state at time t depends on the entire history of the stochastic process. The functional derivative in (3.4) is problematic as it cannot be solved directly. The Hierarchy of Pure states (HOPS) is an alternate approach that removes the presence of this functional integral while simultaneously maintaining the exact dynamics of the system [2].

3.1 Hierarchy Of Pure States

Developing from equation (3.4), to tackle the issue of the functional integral, additional assumptions must be considered. The bath correlation function must be expressed as a sum of exponentials. Finding this representation for the BCF is a non-trivial task which has been investigated in the Hierarchy of Equations of Motion [2]. The expansion of the BCFs takes the form:

$$\alpha(\tau) = \sum_{i=1}^{N} g_i e^{-\omega_i,\tau} \quad \text{with} \quad g_i, \omega_i \in \mathbb{C} \quad \text{and} \quad \tau \geq 0 \tag{3.5}$$

This representation with N exponentials results in N independent auxiliary states. This is simplified by introducing the combined partial derivative:

$$D_\mu^n := \begin{cases} 0 & n = 0 \\ \sqrt{g}_i \sum_{m=0}^{n-1} e^{-\omega_i(n-m)\Delta t}\partial_{z_m^*} & n > 0 \end{cases} \tag{3.6}$$

Here, n and m are discrete-time indices and i is the index from the BCF representation. Inserting the above equation in the NMQSD expression in (3.4) results in:

$$\psi_{n+1} = \psi_n + \Delta t\left(-\mathrm{i}H_{\mathrm{sys}} + \eta_n^* L\right)\psi_n - \Delta t L^\dagger \sum_{\mu=1}^{N} \frac{G_\mu}{\bar{g}_\mu} D_\mu^n \psi_n\,. \tag{3.7}$$

The above expression motivates inserting the main Ansatz of the HOPS method which is the auxiliary states $\psi_n^{\mathbf{k}} := \prod_{\mu=1}^{N}\left(D_\mu^n\right)^{k_\mu}\psi_n$. The total number of iterative applications reflects the order of partial derivatives, referred to as the hierarchy level. With the help of the recursion relation $D_\mu^{n+1} = e^{-W_\mu \Delta t}\left(\bar{g}_\mu \partial_{\eta_n^*} + D_\mu^n\right)$ and inserting it into (3.7):

$$\begin{aligned}\psi_{n+1}^{\mathbf{k}} = \prod_{\mu=1}^{N}\left(D_\mu^{n+1}\right)^{k_\mu}\psi_{n+1} = \prod_{\mu=1}^{N} e^{-k_\mu W_\mu \Delta t}\left(\bar{g}_\mu\partial_{\eta_n^*} + D_\mu^n\right)^{k_\mu} \times \\ \left[1 + \Delta t\left(-\mathrm{i}H_{\mathrm{sys}} + \eta_n^* L - L^\dagger \sum_{\mu=1}^{N}\frac{G_\mu}{\bar{g}_\mu} D_\mu^n\right)\right]\psi_n\end{aligned} \tag{3.8}$$

Keeping only terms up to first order in Δt yields:

$$\begin{aligned}\psi_{n+1}^{\mathbf{k}} = \psi_n^{\mathbf{k}} + \Delta t\left(-\mathrm{i}H_{\mathsf{sys}} - \sum_{\mu=1}^{N} k_\mu W_\mu + \eta_n^* L\right)\psi_n^{\mathbf{k}} \\ - \Delta t L^\dagger \sum_{\mu=1}^{N}\frac{G_\mu}{\bar{g}_\mu}\psi_n^{\mathbf{k}+\mathbf{e}_\mu} + \Delta t L \sum_{\mu=1}^{N} k_\mu \bar{g}_\mu \psi_n^{\mathbf{k}-\mathbf{e}_\mu}\,.\end{aligned} \tag{3.9}$$

To gain the Hierarchy of pure states representation given in [2], $\Delta t \to 0$ must be considered which gives:

$$\dot{\psi}_t^{\mathbf{k}} = (-\mathrm{i}H_{\mathrm{sys}} - \sum_{\mu=1}^{N} k_\mu W_\mu + \eta_t^* L)\psi_t^{\mathbf{k}} + (-L^\dagger)\sum_{\mu=1}^{N} \frac{G_\mu}{\bar{g}_\mu}\psi_t^{\mathbf{k}+\mathbf{e}_\mu} + (L)\sum_{\mu=1}^{N} k_\mu \bar{g}_\mu \psi_t^{\mathbf{k}-\mathbf{e}_\mu} \tag{3.10}$$

Equation (3.10) follows similar stochastic constraints as the NMQSD, namely:

$$\mathcal{M}(\eta_t^*) = 0, \quad \mathcal{M}(\eta_t^*\eta_s^*) = 0 = \mathcal{M}(\eta_t\eta_s), \quad \mathcal{M}(\eta_t\eta_s^*) = \alpha(t-s) \tag{3.11}$$

The structure of the equation (3.10) reveals that an auxiliary state of level $l = \sum_\mu k_\mu$ couples to other auxiliary states with level ± 1 only. Therefore, different states hierarchically depend on each other. To solve this differential equation, the initial conditions need to be specified. By considering that the initial condition for the stochastic pure states coincides with the initial state for the system and the relations shown in the expressions (3.5) and (3.6) at $t = 0$, the initial condition for HOPS are:

$$\begin{aligned} \psi_0^{\mathbf{k}} &= |\psi_0\rangle \quad \text{for k} = 0 \\ \psi_0^{\mathbf{k}} &= 0 \quad \text{for k} \neq 0 \end{aligned} \tag{3.12}$$

In conclusion, based on the exponential representation of the BCF in (3.5), it is shown that the stochastic pure states are equivalently obtained from the HOPS and there is no more functional operator present in this stochastic equation.

3.2 Fermionic Hierarchy of Pure States

After considering a general derivation of the HOPS in the previous section, an important factor is the noise process selected to govern the stochastic dynamics of the modified system. A Gaussian process is implemented but only with the assumption that the constituents follow canonical commutation relations, however, if the system is comprised of particles which do not follow these relations (such as fermions) then not only must a different noise process be considered but the overall HOPS formulation has significant changes.

Considering a Fermionic environment introduced in Fermionic impurity models, only the zero-temperature case with pure initial condition will be considered (The dynamics at the thermodynamic limit will not be considered in this thesis). Rewriting the Hamiltonian (8.14) in the interaction picture, a similar Hamiltonian than in the Bosonic case is gained [2]:

$$\hat{H}_{\mathrm{tot}}(t) = \hat{H}_{\mathrm{s}} + \sum_i (g_i^* e^{i\omega_i t}\hat{c}_i^\dagger \hat{L} + g_i e^{-i\omega_i t}\hat{L}^\dagger \hat{c}_i) \tag{3.13}$$

The Hamiltonian above can be represented in its coherent state using Grassmann variables introduced in an earlier section. These coherent states $|\xi\rangle := \otimes_j \otimes_\lambda |\xi_{j\lambda}\rangle$ are defined by:

$$|\xi_{j\lambda}\rangle = \mathrm{e}^{-\xi_{j\lambda} b_{j\lambda}^\dagger}|0\rangle = |0\rangle - \xi_{j\lambda} b_{j,\lambda}^\dagger |0\rangle \tag{3.14}$$

Here, $\xi_{j\lambda}$ are anti-commutating Grassmann variables which follow standard anti-commutating canonical relations. Using $\psi_t(\xi^*) = \langle\xi|\psi_{\mathrm{tot}}(t)\rangle$ where $|\psi_{\mathrm{tot}}(t)\rangle$ is the total state vector for the system and environment and $\langle\xi|$ is a coherent state representation for the environment. With such a representation, the NMQSD equation for fermionic bath is expressed as [2]:

$$\frac{\partial}{\partial t}\psi_t(\xi^*) = [-i\hat{H}_s + \hat{L}\xi_t^* - \hat{L}^\dagger \int_0^t ds K(t,s)\frac{\delta_l}{\delta\xi_s^*}]\psi_t(\xi^*) \tag{3.15}$$

Where $\xi_t^* = -i\sum_i g_i^* e^{i\omega_i t}\xi_i^*$ is the Grassmann Gaussian noise (Grassmann noise) [2] and $K(t,s) = \sum_i |g_i|^2 e^{-i\omega_i(t-s)}$ is the correlation function. The striking characteristic of the Grassmann noise is that it values anti-commute at different times. The Hamiltonian is now represented as a stochastic Schrodinger quantum state diffusion type equation. Similar stochastic constraints are followed as for the earlier stochastic equations [2]:

$$\mathbb{E}\xi_j^*(t) = \mathbb{E}\left(\xi_j^*(t)\xi_{j'}^*(s)\right) = 0, \quad \mathbb{E}\left(\xi_j^*(t)\xi_{j'}^{*\,*}(s)\right) = \delta_{jj'}\alpha(t-s) \tag{3.16}$$

Analogous to the bosonic case in the earlier section, to express the Hamiltonian into its HOPS representation, auxiliary states of must be defined for the functional derivative in equation (3.15). This hierarchical Ansatz is given by: $\psi_t^{(\boldsymbol{k})} := D_{1,t}^{k_1} D_{2,t}^{k_2} \ldots \psi_t = D_t^k \psi_t$. As shown in [2], the Fermionic hierarchy of pure states equation is given by:

$$\begin{aligned}\partial_t \psi_t^{(\boldsymbol{k})} = &\left(-\mathrm{i}H - \boldsymbol{k}\cdot\boldsymbol{w} + (-1)^{|\boldsymbol{k}|}\sum_j Z_j^*(t)L_j\right)\psi_t^{(\boldsymbol{k})} \\ &+ \sum_j (-1)^{|\boldsymbol{k}|_j} g_j L_j \psi_t^{(\boldsymbol{k}-\boldsymbol{e}_j)} - \sum_j (-1)^{|\boldsymbol{k}|_j} L_j^\dagger \psi_t^{(\boldsymbol{k}+\boldsymbol{e}_j)}\end{aligned} \tag{3.17}$$

A full derivation of equation (3.17) is shown in A1.1

4 Tensor Networks

4.1 Overview of Tensor Network Theory

As mentioned in the introduction, Steve White's density-matrix renormalization group (DMRG) is the most powerful numerical method in the study of one-dimensional quantum lattices [11].

The ground state of a wavefunction for a local Hamiltonian with a gapped ground phase is easier to find due to the entanglement scaling properties. Effective parametrizations allow this corner of the Hilbert space for this simplification and are provided by the matrix product states.

The most common operation in tensor networks is a contraction in which the common dimension of neighbouring tensors is summed over. This generalizes tensor-tensor multiplication. The contraction scheme is not trivial as one deals with larger tensor network representations and is still an active area of research [1].

4.2 Matrix Product States and Matrix Product Operators

The Matrix Product States and Matrix Product Operators allow for a better representation of quantum many-body systems. The main advantages comes with simulating a vector space with a lower dimension than the Hilbert space.

Such a representation can be gained by iteratively 'splitting' the spaces of the Hilbert space in which the quantum state is defined. Given an N-dimensional quantum state $|\psi\rangle = \sum_{j_1,\ldots,j_N}^{d-1} C_{j_1,j_2,\ldots,j_N} |j_1\rangle \otimes \ldots \otimes |j_N\rangle$ which is specified by the knowledge of the rank-N tensor C, splitting the first index from the remaining and performing a singular value decomposition (Schmidt decomposition) [12]:

$$|\psi\rangle = \sum_i \lambda_i |L_i\rangle \otimes |R_i\rangle \tag{4.1}$$

Where λ_i are Schmidt weights and $\{|L_i\rangle\}$ and $\{|R_i\rangle\}$ are the orthonormal sets of vectors. λ is also a diagonal matrix containing the Schmidt weights. It is an important quantity to characterize the entanglement rank [1], which is simply the log of the number of nonzero Schmidt weights, giving the α-Rényi entropy given by [1]:

$$S_\alpha(\rho) = \frac{1}{1-\alpha} log(Tr\rho^\alpha) \tag{4.2}$$

The Von-Neumann entropy is recovered by taking $\alpha \to 0$.

After performing successive singular value decompositions along each cut in the Hilbert space, splitting out the tensor into local tensors and λ, The matrix product state representation is given by contracting the singular value tensors into the local tensors.

An arbitrary many-body state for a system consisting of N subsystems can be written as:

$$|\Psi\rangle = \sum_{l_1,l_2,\ldots,l_N} \Psi_{l_1,l_2,\ldots,l_N} |l_1, l_2, \ldots, l_N\rangle \,, \tag{4.3}$$

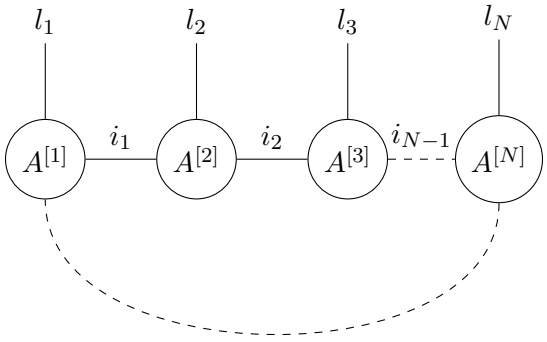

Figure 4.1 Tensor network diagram for the MPS representation of the state in equation (4.4) Each circle represents a tensor $A^{[i],l_i}$ with physical index l_i and virtual indices i_j. The dashed line indicates periodic boundary conditions, forming a closed chain.

Where the multi-mode states are basis vectors of the many-body Hilbert space and the coefficients are scalars indexed for the respective mode in the state space. This can be further expressed as a MPS by:

$$\begin{aligned} |\Psi\rangle &= \sum_{l_1,l_2,\ldots,l_N} \sum_{i_0=1}^{\chi_0} \sum_{i_1=1}^{\chi_1} \cdots \sum_{i_{N-1}=1}^{\chi_{N-1}} A^{[1],l_1}_{i_0,i_1} A^{[2],l_2}_{i_1,i_2} \cdots A^{[N],l_N}_{i_{N-1},i_0} |l_1, l_2, \ldots, l_N\rangle \\ &= \sum_{l_1,l_2,\ldots,l_N} \operatorname{tr}\left(\mathbf{A}^{[1],l_1}\mathbf{A}^{[2],l_2}\cdots\mathbf{A}^{[N],l_N}\right) |l_1, l_2, \ldots, l_N\rangle\,, \end{aligned} \tag{4.4}$$

The construction in (4.4) is both general and exact. While SVD is used to gain such a representation, it is sometimes tedious to perform [12]. A numerically cheaper technique which can be used is the QR decomposition [11], where an arbitrary matrix M of dimension (n_a, n_b) is decomposed into $M = QR$, Where Q has dimension (n_a, n_a) and is unitary while R has dimension (n_a, n_b) and is upper triangle.

An MPS is an extension of the concept of tensor contraction where each tensor represents a single site. Each tensor has a physical dimension which points outward into which local operators, can be contracted into the site. Downward-facing physical dimensions represent a ket state and upwards are either a bra state or a conjugate state. Since exponential growth is a hindrance to scaling tensor networks. It is known that truncating these bond dimensions results in a good approximation of a state and reduces the bond dimension as much as possible through singular-value decomposition [11].

Each tensor sit can be further expressed as a canonical form. A canonical form can be identified if the contraction along the specific dimensions results in the identity. The main advantage of this is a speedup in the convergence of the algorithm [11]. A tensor can be in left canonical or right canonical form which relates to which contractions lead to the identity represented by a single line in tensor network notation.

A Matrix product state has bounded levels of entanglement [6], which are manifested as area laws. Gauge fixing is a method used to improve the numerical stability of performing calculations using MPS and is also a standard method to initialise a MPS chain before performing very common time-evolving algorithms such as DMRG, TEBD and TDVP [12].

Gauge transformations, which are certain transformations that can be performed upon an MPS which leave the physical state that it is representing to be invariant, correspond to basis transformations on a virtual level. These transformations can then be "blocked", which is a process that combines a chain of MPS tensors into a single effective tensor on a larger physical region. This procedure leaves the initial MPS in its canonical form. The gauge transformation is usually done by performing an SVD or a QR decomposition on each tensor site.

Although gauge degrees of freedom can be manipulated to set a chosen tensor A_j as a centre of orthogonality, this does not fully fix this degree of freedom on any of the links between the tensor since the tensor A_j will remain a centre of orthogonality under a unitary change of gauge (the gauge change is implemented by a unitary matrix and its hermitian conjugate). If an additional constraint on the link is that it is diagonal with positive elements in ascending order, this completely fixes the gauge freedom of the link solving the earlier problem. By setting every link of a tensor chain as a centre of orthogonality, the new form of the MPS is called the canonical form. The uniqueness of this property follows from the correspondence between the link-based centre of orthogonality and the SVD [5].

A common canonical form to bring a MPS into is the left-isometric/canonical form:

$$\sum_{j=0}^{d-1} A_j^\dagger A_j = 1_{D\times D} \tag{4.5}$$

Putting an MPS in this form is known as partial gauge fixing [11]. Putting an MPS into its left and right isometric form creates a centre of orthogonality. This is determined if every branch attached to a specific tensor site A_j forms an isometry between its open indices and the index connected to tensor A_j [11]

The compact expression after bringing the MPS into a canonical form can be:

$$|\psi(A)\rangle = \sum_i v_L^\dagger [\Pi_{n\in\mathbb{Z}} A^{i_n}] v_R |i\rangle \tag{4.6}$$

Where A^i is a $D \times D$ matrix for every entry of the index i [11]. A can be seen as a three-index tensor of dimensions $D \times d \times D$, where d is the dimension of the physical Hilbert space at every site in the chain and D is the bond dimension.

Operators can also be written in the MPS formalism. A general operator acting on a many-body system can be written as :

$$\hat{H} = \sum_{l_1,l_2,\ldots,l_N} \sum_{l_1',l_2',\ldots,l_N'} H_{l_1,l_2,\ldots,l_N}^{l_1',l_2',\ldots,l_N'} |l_1, l_2, \ldots, l_N\rangle\langle l_1', l_2', \ldots, l_N'| \tag{4.7}$$

From the area law, the MPS form a vanishingly small corner of the full Hilbert space, and thus cannot be them to approximate arbitrary quantum states

4.3 Time Dependent Variational Principle

Many tensor network algorithms work by sweeping across the chain of sites. Splitting the infinite/finite chain into left-canonical and right-canonical forms allows operations to focus purely on that site known as the orthogonality centre.

The properties and geometry of both the parameter space within which the MPS lies and its corresponding manifold in Hilbert space are used to define the necessary steps for performing the time evolution of the quantum state as a tensor network. This is known as the Time Dependent Variational principle (TDVP) and is the main approach used in this thesis.

Implementing the TDVP algorithm to simulate the time evolution of Hamiltonians can be done without an increase in computational cost [13], resulting in a relatively quick convergence, without violating energy conservation for constant Hamiltonians or any other conservation laws dictated by the symmetries within

the Hamiltonian.

One first interprets the set of MPS with a determined bond dimension as a manifold within the Hilbert space in which the wavefunction is represented in. This manifold is defined by mapping the set of $D \times d \times D$ tenors A and physical states in the Hilbert space $|\psi(A)\rangle$ [13]. The resulting manifold is not a linear subspace as the sum of two MPS with the same bond dimension is not in the same manifold. Therefore, considering the tangent space consisting of taking the tangent of every point in the wave function $|\psi(A)\rangle$.The Schrodinger equation can be expressed as:

$$i\frac{\partial}{\partial t}|\psi(A)\rangle = H|\psi(A)\rangle \tag{4.8}$$

Which determines how a quantum state evolves in time within a manifold. The overlap between the two tangent vectors introduces an important metric on the tangent space known as the Gram matrix, given by:

$$\langle\psi(\bar{B'};\bar{A})\psi(B;A)\rangle = \bar{B}^{i,}G_{ij}(\bar{A},A)B^{j} \tag{4.9}$$

Where $G_{ij}(\bar{A},A) = \langle\partial_i\psi(\bar{A})|\partial_j\psi(A)\rangle$ is the Gram matrix.

The main issue with equation (4.8) is that the initial MPS $|\psi(A)\rangle$ is immediately taken out of the manifold. To determine the time evolution of the state in the manifold $|\psi(A(A))\rangle$, the time derivative is given as:

$$i\frac{\partial}{\partial t}|\psi(A)\rangle = |\psi(\dot{A};A)\rangle \tag{4.10}$$

Which is a tangent vector. Finding $\dot{A}$ which provides the best approximation to $H|\psi(A(A))\rangle$ results in the minimization problem:

$$\dot{A} = \arg\min_{B} \| H\,|\Psi(A)\rangle - |\Phi(B;A)\rangle\|_2^2 . \tag{4.11}$$

The solution to the minimization problem (4.11) can be solved similarly by taking the projection of equation (4.10), which projects the linear Schrodinger equation into a non-linear differential equation manifold [13]. which is given as:

$$i\frac{\partial}{\partial t}|\psi(A)\rangle = P_{A(t)}H|\psi(\dot{A};A)\rangle \tag{4.12}$$

The TDVP equation is then written as:

$$\begin{aligned} i\frac{\partial}{\partial t}\,|\Psi(A)| &= \left(\partial_{A_i}\,|\Psi(A)\rangle\right)(G^{-1})^{ij}\left(\partial_{\bar{A}_i}\left\langle\Psi(\bar{A})\right|\right)H\,|\Psi(A)\rangle \\ &= \partial_{A_i}\,|\Psi(A)\rangle\,(G^{-1})^{ij}\partial_{\bar{A}_j}h(A,\bar{A}), \end{aligned} \tag{4.13}$$

Where $h(A,\bar{A}) = \langle\psi(\bar{A})|H|\psi(A)\rangle$. The TDVP equation (4.12) can be expressed in the uniform gauge.

The procedure for computing the time derivative of the MPS tensor A according to the TDVP can be followed in [13]. The simplest option is performing an Euler decomposition for the differential equation for $A(t)$ which is given as $A(t+\delta t) = A(t) + \delta t\dot{A(t)}$. A numerical integrator that does not have the symplectic properties of the TDVP equation is also preferred, such as Runge-Kutta [12]. In the Hilbert space, the imaginary time evolution of a state $|\psi_0\rangle$ results in a projection onto the ground state in the infinite-time limit [13]:

$$\lim_{\tau\to}\frac{e^{-H\tau}|\psi\rangle}{||e^{-H\tau}|\psi\rangle||} = |\psi_0\rangle \tag{4.14}$$

The Euler scheme to integrate the differential equation to solve for the tensor operator $\dot{A}$ is similar to performing a steepest-descent optimization with a tangent-space gradient [13].

5 Hierarchy of Matrix Product States

5.1 HOMPS Ansatz

The hierarchy of matrix product states (HOMPS) representation of the HOPS algorithm allows for a tensor network representation for the impurity Hamiltonian. The first step is to express the standard Hamiltonian into an effective stochastic Hamiltonian defined by [3], which is:

$$\hat{H_{eff}} = \hat{H}_S + i\hat{L}Z_t^* - i\sum_{k=1}^{K} v_k \hat{b_k^\dagger}\hat{b_k} - i\hat{L^\dagger}\sum_{k=1}^{K}\sqrt{|d_k|}\hat{b_k} + i\hat{L}\sum_{k=1}^{K}\frac{d_k}{\sqrt{|d_k|}}\hat{d_k^\dagger} \tag{5.1}$$

Similar notation follows from the hierarchy of pure states, the statistics of the operators and the noise process depend on whether the bath consists of fermions or bosons. The parameter d_k is a scaling parameter which could be understood as a means to improve the numerical stability of HOMPS. The creation and annihilation operators are acted upon a basis state of $\{n_k\}$ where k is the hierarchy index and it plays the role of occupation numbers. Such an expression allows for a MPS representation to be developed. The HOPS systems of equations shown in (3.10) can be expressed for a wave function:

$$|\psi(Z^*)\rangle_t = \sum_n \psi_t^n(Z^*)|\mathrm{n}\rangle \tag{5.2}$$

as

$$\partial_t|\psi(Z^*)\rangle_t = -i\hat{H}_{eff}(Z^*)|\psi(Z^*)\rangle_t \tag{5.3}$$

The product of sums in equation (5.1) can be implemented in terms of MPS and MPO [3]. The wave function (5.2) is first represented as an MPS by expanding $|\psi\rangle_t$ on a product of system states $|l\rangle$ and the introduced pseudo-Fock states:

$$|\psi\rangle_t = \sum_{l,n}\psi_t^{l,n}|l,n_1,\ldots,n_K\rangle = \sum_{l,n,a} A^l_{1,a_0}A^{n_1}_{a_0,a_1}\ldots A^{n_K}_{a_{K-1},a_1}|l,n_1,\ldots,n_K\rangle \tag{5.4}$$

Each $A^{n_i}_{a_{i-1},a_i}$ is a rank-tensor with one physical index, which is determined by the Hierarchy, and two virtual indices, whose ranges are determined by the bond dimensions. In the MPS, the physical bond dimension n_k represents the original indexing of the HOPS. Furthermore, an MPO representation can be gained through:

$$\hat{H_{eff}} = \sum_{l,l',n,n',w} W^{l,l'}_{1,w_0}W^{n_1,n_1^{'}}_{w_0,w_1}\ldots W^{n_K,n_K^K}_{w_{K-1},1}|l,n_1,\ldots,n_K\rangle\langle n_K^{'},\ldots,n_1^{'},l'| \tag{5.5}$$

Where the MPO $W^{n_i,n_i^{'}}_{w_{i-1},\ldots,w_i}$ represents the matrix of local operators acting on the ith effective mode [11]. This representation gives the so-called Hierarchy of Matrix Product states construction from the wave function. This can be achieved using the state machine method to construct this MPO [3]. It becomes numerically stable to truncate the MPO order for numerical stability. Better numerical results can be achieved by rescaling the HOPS proposed in [3].

5.2 Implementing HOMPS

To gain a matrix product operator representation of equation (3.10), one can start by representing the full hierarchy at time t by a single quantum state:

$$|\Psi_t\rangle = \sum_{l,\mathbf{n}} \Psi_t^{l,(\mathbf{n})}\,|l,n_1,n_2,\ldots,n_K\rangle\,, \tag{5.6}$$

For basis states which are tensor products of system states $|l\rangle$ and auxiliary "pseudo-Fock" states $|n\rangle$. To obtain a "Pseudo-Fock" representation of the wavefunction in equation (3.10), the ladder operators in equation (5.7) must be defined and inserted into the effective stochastic Hamiltonian in (3.17).

$$\begin{aligned} \hat{b}_k'^{\dagger} |\mathbf{n}\rangle &:= \sqrt{n_k + 1}\, |\mathbf{n} + \mathbf{e}_k\rangle\,, \\ \hat{b}_k' |\mathbf{n}\rangle &:= \sqrt{n_k}\, |\mathbf{n} - \mathbf{e}_k\rangle\,, \\ \hat{N}_k |\mathbf{n}\rangle &:= n_k\, |\mathbf{n}.\rangle \end{aligned} \tag{5.7}$$

Which are used to update the full state given by equation (5.3) with the stochastic effective Hamiltonian (5.1). To get an MPO representation for equation (5.5), the finite state machine algorithm can be used [14]. Using this approach, the MPO gained from equation (5.1) is represented as:

$$\begin{aligned} \boldsymbol{W}^{[1]\prime} &:= \begin{pmatrix} -i\mathbb{I} & i\hat{L} & i\left(\hat{L}^{\dagger}\right) & \hat{H}_S + i\hat{z}_t^* \hat{L} \\ 0 & 0 & 0 & 0 \\ 0 & 0 & 0 & 0 \\ 0 & 0 & 0 & 0 \end{pmatrix}, \\ \boldsymbol{W}^{[k+1]\prime} &:= \begin{pmatrix} \mathbb{I} & 0 & 0 & \omega_k \hat{N}_k \\ 0 & \mathbb{I} & 0 & \frac{-d_k}{\sqrt{|d_k|}} b_k'^{\dagger} \\ 0 & 0 & \mathbb{I} & \sqrt{|d_k|}\hat{b}_k' \\ 0 & 0 & 0 & \mathbb{I} \end{pmatrix}, \quad k = 1, 2, \ldots, K, \end{aligned} \tag{5.8}$$

The expectation values for a physical observable $L^{\dagger}$ can be calculated as:

$$\begin{aligned} \left\langle \hat{L}^{\dagger} \right\rangle_t &= \frac{\langle \Psi_t^{(0)} | \hat{L}^{\dagger} | \Psi_t^{(0)} \rangle}{\langle \Psi_t^{(0)} | \Psi_t^{(0)} \rangle}, \\ |\Psi_t^{(0)}\rangle &= \sum_{l,i} A^{[1],l}_{i_0,i_1} A^{[2],0}_{i_1,i_2} A^{[3],0}_{i_2,i_3} \ldots A^{[K+1],0}_{i_K,i_0} |l\rangle. \end{aligned} \tag{5.9}$$

6 Grassmann Tensor Networks

Developing from the MPS representation introduced in the previous sections, the framework for Grassmianian tensor networks, which (in this thesis) is an MPS chain where each site represents a state in the Grassmann representation. The formalism for Grassmann tensor networks will first be introduced and then it will later be applied to the context of fermionic coherent states.

6.1 Grassmann Tensor Product States

Using variables $\eta_{i;1,\ldots,N}$ as single-component Grassmann numbers can be considered as links to their respective coefficient tensors $T_{i_1,\ldots,i_N}$ with rank N. The Grassmann tensor of rank N can then be expressed as [7]:

$$T_{\eta_1\eta_2\cdots\eta_N} = \sum_{i_1=0}^{1}\sum_{i_2=0}^{1}\cdots\sum_{i_N=0}^{1} T_{i_1 i_2\cdots i_N}\eta_1^{i_1}\eta_2^{i_2}\cdots\eta_N^{i_N} \tag{6.1}$$

These tensor networks follow similar properties of a standard MPS chain, such as contraction and reshaping, however, additional considerations due to the anti-commutation relation of the Grassmann links must be made, as this will result in a sign change. Two Grassmann tensors of rank N and M $A_{\eta_1,\ldots,\eta_N}$ and $B_{\zeta_{1,\ldots,\zeta_M}}$ respectively can be contracted from η_1 to ζ_i as:

$$\int \mathrm{d}\bar{\xi}\mathrm{d}\xi \mathrm{e}^{-\bar{\xi}\xi}\mathcal{A}_{\xi\eta_2\ldots\eta_N}\mathcal{B}_{\bar{\xi}\zeta_2\ldots\zeta_M}. \tag{6.2}$$

Which is itself a Grassmann tensor. This contraction can be computed as:

$$C_{i_1,\ldots,i_N} = \sum_{i_i}^{N} A_{i_2,i_3,\ldots,i_n}B_{i_2,i_3,\ldots,i_N}s_{i_2,\ldots,i_N} \tag{6.3}$$

Where $s_{i_2,\ldots,i_N}$ is the sign factor tensor which considers the anti-commutating relations between the Grassmann indices and is expressed as:

$$s_{i_2,\ldots,i_N} = \Pi^{i_1,i_2,\ldots,i_N} \times (-1)^{P(L)*(\sum_{i>i_1}^{N}P(i))+\Pi_{i>2}^{N}(P(i))} \tag{6.4}$$

Where $P(i)$ is the parity function which converts the composite index i to binary. The sign factor tensor must be recalculated and rewritten for every contraction [7]. Numerically, these tensors were simulated using the GrassmannTN python package [15] for this thesis.

6.2 GrassmannTN: A Python Library

This section will cover the fundamentals from a Python library called GrassmannTN [15], which allows a user to efficiently simulate Grassmann tensor networks. This is also the library used to implement HOGTPS,however, due to timing constraints, no results were gained. Regardless, the formalism and structure of [15] is discussed here to show how a stochastic Hamiltonian of the form (5.1) with Grassmann generators can be implemented.

6.2.1 Contracting Grassmann Tensors

A generic Grassmann tensor encodes 4 types of information [7], the numerical coefficient tensor T, the statistics of the indices, the index encoding method and the coefficient format, expressed as:

$$T_{\psi_1,\ldots,\psi_m,\zeta_1,\ldots,\zeta_m} = \sum_{I_1,\ldots,I_m J_1,\ldots,J_n} T_{I_1,\ldots,I_m J_1,\ldots,J_n} \psi_1^{I_1} \ldots \psi_m^{I_m} \zeta_1^{J_1} \ldots \zeta_m^{J_m} \tag{6.5}$$

Describing these terms in a bit more detail, the statistics determine to the type of index on each site which can be: +1 (non-conjugate fermionic index), -1 (conjugate index) and 0 (bosonic index). This can be further represented diagrammatically by considering the non-conjugate fermionic index to be presented as a tensor leg with an arrow pointing from the tensor, the conjugate fermion index as a tensor leg with an arrow pointing into the tensor and bosonic tensors having no arrow. The index encoder refers to how a composite index $I = (i_1, \ldots, i_n)$ is encoded as an integer. The two options are parity-preserving and canonical encoders as shown in [7].

The advantage of the canonical encoder is that it is relatively easier to join and split tensor indices. The parity-preserving encoder is designed to readily manifest the Grassmann parity of the specific index [7].

The two conditions which must be met before contracting two Grassmann tensors are that they must have the same dimension and have the opposite statistics. The contraction between two Grassmann tensors $A_\psi = \sum_I A_I \psi^I$ and $B_\zeta = \sum_J B_J \zeta^J$ can be calculated as:

$$\int_{\psi\zeta} A_\psi B_\zeta = \sum_{\{i\}} (\Pi_{a>b} (-1)^{i_a i_b}) A_{i_1 \ldots i_n} B_{i_1 \ldots i_n} = \sum_I \sigma_I A_I B_I \tag{6.6}$$

6.2.2 Joining and Splitting Grassmann Tensors

Grassmann tensors can also be reshaped similarly to traditional tensors, however, the process of joining and splitting tensor legs introduces an additional sign factor to the coefficient tensor T which must be considered. This can be understood in algebraic terms as joining the Grassmann algebra encoded on each leg into a single Grassmann algebra. This is done in two steps [5], first by combining the algebras using a direct sum and finally forming the resulting Grassmann algebra (m) into a graded tensor product of t:

$$t = v_1 \oplus \ldots \oplus v_m \oplus u_1 \oplus \ldots u_n \quad ; \quad m = \mathbb{C} \oplus \mathfrak{t} \oplus (\mathfrak{t} \otimes \mathfrak{t}) \oplus \cdots \oplus \underbrace{(\mathfrak{t} \otimes \mathfrak{t} \otimes \cdots \mathfrak{t})}_{m+n}. \tag{6.7}$$

The first equation in (6.7) represents the direct sum of the Grassmann algebra, and the second equation in (6.7) forms the resulting direct sum into graded tensor products. The process of joining Grassmann algebras is useful when considering reshaping the Grassmann tensors as well.

6.2.3 Grassmann Tensor Decomposition

Similar to the SVD method mentioned earlier for generic tensors, Grassmann tensors can be decomposed using singular values [7];

$$M_{\psi,\phi} = \int_{\bar{\eta}\eta,\bar{\zeta}\zeta} U_{\bar{\psi}\eta} \Sigma_{\bar{\eta}\zeta} V_{\bar{\zeta}\phi} \tag{6.8}$$

Where U and V are unitary matrices and $\sum_{e\bar{t}a\zeta} = \sum_I \lambda_I \sigma_I \bar{\eta}^I \zeta^I$ is the singular value matrix. For a general Grassmann tensor network, the SVD decomposition can be expressed as:

$$T_{\psi_1 \cdots \bar{\phi}_1 \cdots i_1 \cdots \psi_1' \cdots \bar{\phi}_1' \cdots k_1 \cdots} = \int_{\bar{\eta}\eta,\bar{\zeta}\zeta} U_{\psi_1 \cdots \bar{\phi}_1 \cdots i_1 \cdots \eta} \Sigma_{\bar{\eta}\zeta} V_{\bar{\eta}\psi_1' \cdots \bar{\phi}_1' \cdots k_1 \cdots}, \tag{6.9}$$

Where $\Sigma_{\bar{\eta}\zeta}$ is, just as before, the diagonal singular value matrix.

As mentioned earlier in this section, the initialization and operations of Grassmann tensors are performed using the GrassmannTN python package [15].

6.3 Fermion Coherent State Representation of GTPS

A simple Grassmann tensor network representing an electron-level filling state can be given as [8]:

$$\psi_f(\{m_i\}) = \int \Pi_i T_i^{m_i} \Pi_{ij} G_{ij} \tag{6.10}$$

Where the tensors $T_i^{m_i}$ and G_{ij} are compact representations of the Grassmann components within the tensor network, given as:

$$T_i^1 = d\theta_i, \quad T_i^0, \quad G_{ij} = 1 + u_{ij\theta_i\theta_j} \tag{6.11}$$

Where θ_i are the Grassmann numbers acting on site i introduced in the earlier section. The integral $\in$ is the Berezin integral and it only integrates the Grassmann numbers. Tensors $T_i^{m_i}$ can be understood as a dimension-1 tensor and G_{ij} as a dimension-1 rank 2 tensor on site ij

A Fock basis representation also exits [16] and is straightforward to derive, however, due to the anti-commutating relations for different Grassmann numbers, the ordering for different local Grassmann tensors $T^{m_i}_{i;a_k,a_l,\ldots}$, must always be checked, which negatively influences the numerical simulation of such a tensor network. A Fermionic coherent representation is shown in [8], where the basis of the fermionic wave-functions is independent of the ordering of local Grassmann tensors, addressing the numerical simulation issue. A fermionic tensor product state can be expressed as:

$$|\psi\rangle = \sum_{\{m_i\}} \sum_{\{a_I\}} \int \Pi_i [c_i^\dagger]^{m_i} T^{m_i}_{i;a_k,a_l,\ldots} \Pi_{ij} G_{ij,a_I a_J} |0\rangle \tag{6.12}$$

Where $m_i = 0, 1$ represents the fermionic occupation numbers which are conserved through Pauli's exclusion principle. The Grassmann tensor product wave function can be derived under the Fock basis:

$$|Pi_i (c_i)^{m_i}|0\rangle = (c_1^\dagger)^{m_1} (c_2^\dagger)^{m_2} \ldots |0\rangle \tag{6.13}$$

Implementing the over complete fermion coherent state basis:

$$|\eta\rangle = \Pi_i (1 - \eta_i c_i^\dagger)|0\rangle \tag{6.14}$$

By using the closure relation:

$$\Pi_i d\eta_i^* d\eta_i (1 - \eta_i^* \eta_i)|\eta\rangle\langle\eta| = 1 \tag{6.15}$$

The matrix Grassmann tensor product can be achieved for an arbitrary fermionic MPS tensor:

$$\langle\eta|\eta\rangle = \sum_{\{m_i\}} \sum_{\{a_I\}} \int \Pi \eta_i^{m_i} T^{m_i}_{i;a_k a_L} \Pi_{ij} G_{ij;a_I a_J} \tag{6.16}$$

A cleaner expression can be gained if the Grassmann tensor $T^{m_i}_{i;a_k,a_l}, \ldots$ is redefined as:

$$T^{m_i}_{i;a_k,a_l,\ldots} = \sum_{\{l_K^{a_K}\}\{l_L^{a_l}\}} T^{m_i;\{l^{a_K}\}\{l_L^{a_L}\}}_{i;a_k,a_l,\ldots} \eta_i^{*m_i} \Pi_{I\in i} \Pi_{a_I} (d\theta_I^{a_I})^{l_I a_I} \tag{6.17}$$

The wavefunction can then be expressed as:

$$\psi(\eta^*) = \sum_{\{m_i\},\{a_I\}} \int \Pi_i T^{m_i}_{i;a_k,a_l,\ldots} \Pi_{ij} G_{ij;a_I a_J} \tag{6.18}$$

The main advantage of the newly expressed wave function $(6.18))$ is that it always contains an even number of Grassmann numbers [16], therefore, this wavefunction is completely independent of the ordering of those local Grassmann tensors $T^{m_i}_{i;a_k,a_l,\ldots}$, which significantly improves the simulation efficiency for such tensor networks. Another advantage of expressing the wave function in the representation (6.18) is the convenience of calculating local physical quantities [7]. The norm of this tensor product can be expressed as a tensor trace of Grassmann tensor network and other local physical quantities such as energy can be expressed as a trace of Grassmann tensor networks. The norm of the wave function (6.18) is calculated as:

$$\int \Pi_i \mathrm{d}\eta_i^* \eta_i (1-\eta_i^* \eta_i) \psi^* \eta \psi^* \eta^* = \sum_{\{p_I\}} \int \Pi_i T_{i;p_K p_L \ldots} \Pi_{ij} G_{ij;p_I p_J} \tag{6.19}$$

For local operators containing $c^\dagger$ and c, these terms need to be mapped to Grassmann numbers and integrated using the Berezin integral with respect to a proper measure. An example of calculating the norm of the fermion occupation number is shown in A1.2

Performing standard tensor network operations on Grassmann tensor networks follows similar methodologies, however, additional considerations arising from the anti-commuting variables and the nature of Grassmann variables must be considered as well. A few of these operations which are important for the next section will be introduced here.

7 Hierarchy of Grassmannian Tensor Product States

In the HOMPS ansatz (5.2), pseudo-occupation states were defined as the basis for developing a matrix product state/operator ansatz. It was seen earlier that a similar type of matrix product state can be developed from a set of Grassmann generators in section (1). Similarly, one can introduce pseudo-Grassmannian generators to reformulate the HOPS ansatz as a Grassmann tensor product state.

The main goal is the express the fermionic hierarchy of pure states Ansatz (3.17) into a tensor product state. This was difficult to do earlier as the FHOPS is expressed in the Grassmann basis satisfying Grassmann algebra and a matrix representation was not trivial to obtain. However, as seen in the "Grassmann Tensor Network" section, the Grassmann generators are considered as the links in the tensor network. The fermionic coherent state representation for Grassmann tensor networks $(6.12$) can be used as an alternative approach as an Ansatz [8], however, a more general Ansatz will be used (6.5). The former will be more advantageous numerically as this formulation immediately has an even number of Grassmann generators. However, the simplicity in coding the Ansatz (6.5) is preferred.

The formulation is straightforward, developing further from the HOMPS Ansatz (5.2) by using the generalized Weyl-Heisenberg algebra (2.16), the Fock states can be represented by Grassmann generators. First we represent the "pseudo"-Fock states in the fermionic basis:

$$\begin{aligned} \hat{c}_k'^{\dagger} |\mathbf{n}\rangle &:= (-1)^{\sum_{l<k} n_l} \cdot (1-n_k) |\mathbf{n}+\mathbf{e}_k\rangle , \\ \hat{c}_k' |\mathbf{n}\rangle &:= (-1)^{\sum_{l<k} n_l} \cdot n_k |\mathbf{n}-\mathbf{e}_k\rangle , \\ \hat{N}_k |\mathbf{n}\rangle &:= \hat{c}_k \hat{c}_k^{\dagger} |\mathbf{n}\rangle := n_k |\mathbf{n}.\rangle \end{aligned} \tag{7.1}$$

Where $\hat{c}_k$ and $\hat{c_k}^{\dagger}$ are fermionic creation and annihilation operators. After expressing the FHOPS (3.17) into the HOMPs ansatz for pseudo-Fock states $\{|\mathbf{n}\rangle\}$ with $|\mathbf{n}\rangle = |n_1, \ldots, n_K\rangle$ and in the fermionic basis as in equation (7.1). Following the same recipe as in [3] for bosonic operators. can be followed for fermionic operators. The following effective stochastic Hamiltonian is achieved, gaining a fermionic hierarchy of matrix product states (FHOMPS) Ansatz:

$$\hat{H}_{\text{eff}} = \hat{H}_{\text{S}} + i\hat{L}Z_t^* - i\sum_{k=1}^{K} \nu_k \hat{c}_k^{\dagger}\hat{c}_k \quad -i\hat{L}^{\dagger}\sum_{k=1}^{K} \sqrt{|d_k|}\hat{c}_k + i\hat{L}\sum_{k=1}^{K} \frac{d_k}{\sqrt{|d_k|}}\hat{c}_k^{\dagger} \tag{7.2}$$

Z_t^* is the stochastic Grassmanian noise ($Z_t^* = -i\sum_i g_i^* e^{i\omega_i t}\partial/\partial\eta_i$). From [4], the Grassmann algebra is isomorphic to the algebra of creation and annihilation operators for fermions with the following correspondence:

$$c_i^{\dagger} \mapsto \eta_i \ , \quad c_i \mapsto \partial/\partial\eta_i \tag{7.3}$$

Using this correspondence, a quick mapping can be performed to represent the FHOMPS Ansatz in terms of Grassmann generators. This expresses the effective stochastic Hamiltonian as :

$$\hat{H}_{\text{eff}} = \hat{H}_{\text{S}} + i\hat{L}Z_t^* - i\sum_{k=1}^{K} \nu_k \eta_k \frac{\partial}{\partial\eta_k} - i\hat{L}^{\dagger}\sum_{k=1}^{K} \sqrt{|d_k|}\frac{\partial}{\partial\eta_k} + i\hat{L}\sum_{k=1}^{K} \frac{d_k}{\sqrt{|d_k|}}\eta_k \tag{7.4}$$

Using the correspondence defined in equation (2.20), a non-conjugate Grassmann polynomial (η_i) results in increasing the total number of Grassmann generators by one and a differential Grassmann operator ($\partial/\partial\eta_i$) results in decreasing the total number of Grassmann generators by one.

$$c_i^\dagger|\mathrm{n_i}\rangle \mapsto e_{n+1}(\vec{\theta_{l_i}}) \ , \quad c_i|\mathrm{n_i}\rangle \mapsto e_{n-1}(\vec{\theta_{l_i}}) \tag{7.5}$$

Where n is the total number of elements in the pseudo-Fock space in the fermionic basis in equation (7.1) and $\vec{\theta} = (\theta_{i_1}, \theta_{i_2}, \ldots, \theta_{i_n})$. The effective stochastic Hamiltonian can now be expressed in terms of raising and lowering Grassmann generators:

$$\begin{aligned}\hat{H}_{\mathrm{eff}} = \hat{H}_{\mathrm{S}} + i\hat{L} - i\sum_i g_i^* e^{i\omega_i t}\cdot e_{n-1}(\vec{\theta_{l_i}}) - i\sum_{k=1}^{K}\nu_k e_{n+1}(\vec{\theta_{l_i}})\cdot e_{n+1}(\vec{\theta_{l_i}}) \\ -i\hat{L}^\dagger\sum_{k=1}^{K}\sqrt{|d_k|}e_{n-1}(\vec{\theta_{l_i}}) + i\hat{L}\sum_{k=1}^{K}\frac{d_k}{\sqrt{|d_k|}}e_{n+1}(\vec{\theta_{l_i}})\end{aligned} \tag{7.6}$$

The Grassmann generators here serve as links within the Grassmann tensors network and the coefficients in (7.4) become the coefficient tensors in (6.5). The expression in (7.4) assumes that the system Hamiltonian $\hat{H}_S$ is bosonic, however, if the system Hamiltonian contained fermionic terms, a similar mapping (7.3) can be used.

The Hamiltonian in equation (7.6) can be efficiently coded symbolically using GrassmannTN [15]. Using this library, a matrix representation of equation (7.6) can be achieved, converting the symbolic Grassmann expressions into a matrix format representing the Fermionic basis while considering the parity sign of each matrix element, giving a form similar to the MPS equation (5.6). The finite state machine algorithm could also be applied to equation (7.4) to gain a Grassmann tensor product operator. This will give a form:

$$\begin{aligned}\boldsymbol{W}^{[1]\prime} &:= \begin{pmatrix} -i\mathbb{I} & i\hat{L} & i\left(\hat{L}^\dagger\right) & \hat{H}_S + \sum_i g_i^* e^{i\omega_i t}\partial/\partial\eta_i\cdot\hat{L} \\ 0 & 0 & 0 & 0 \\ 0 & 0 & 0 & 0 \\ 0 & 0 & 0 & 0 \end{pmatrix}, \\ \boldsymbol{W}^{[k+1]\prime} &:= \begin{pmatrix} \mathbb{I} & 0 & 0 & \omega_k\eta_k\frac{\partial}{\partial\eta_k} \\ 0 & \mathbb{I} & 0 & \frac{-d_k}{\sqrt{|d_k|}}\eta_k \\ 0 & 0 & \mathbb{I} & \sqrt{|d_k|}\frac{\partial}{\partial\eta_k} \\ 0 & 0 & 0 & \mathbb{I} \end{pmatrix}, \quad k = 1, 2, \ldots, K,\end{aligned} \tag{7.7}$$

The MPO in (7.7) assumes that the system Hamiltonian $\bar{H_S}$ consists of bosonic operators (bosonic system). An alternative approach for The TDVP algorithm can be directly performed on Hamiltonian (7.6) after it is first expressed symbolically using GrassmannTN [15]. The sign factor must be considered after contracting, splitting or joining the Grassmann tensors. I attempted this approach to simulate (7.6), however, as mentioned earlier, timing restrictions didn't allow any further progress.

This approach can be used to simulate open quantum systems consisting of either fermionic/bosonic baths or system Hamiltonian, even a hybrid mix of fermionic bath and bosonic system. Obtaining numerical results to benchmark the stochastic Hamiltonian in equation (7.4) will be the next step in the future.

8 Quantum Impurity Models and Implementing HOMPS

The general class of quantum impurity models describes a localized, discrete quantum system [17]. The impurity is coupled to a bath, which is a noninteracting excitation with a continuous (non-discrete) excitation spectrum. The initial motivation to develop quantum impurity models was to explain certain anomalies in the resistivity of magnetic alloys [18].

These models have now become ubiquitous in current-day research, especially in quantum technologies. One of the reasons is that the impurity can be considered classified as a quantum system of interest itself, a component of a quantum-sensing device or act as a scatterer in a host material [19], [20]. Major research goals are the dynamical and coherent control and read-out of their quantum state and the minimization of decoherence effects due to their coupling with the environment. An example of such an experimental realization is considering impurities as quantum sensors to read out properties of nearby quantum systems with high sensitivity [20].

A second motivation to investigate quantum impurity models is that they are perfect testbeds for analytical and numerical techniques in quantum many-body physics [17]. Few-level quantum impurity systems coupled with infinitely many environmental degrees of freedom are often suitable starting points to develop, test and compare different analytical and numerical approaches.

An initial Hamiltonian used to describe such an impurity system was proposed originally by Feynmann and Vernon [21], where they described the environment in terms of a bath of harmonic oscillators as shown in equation (8.1).

$$\hat{H} = -\hat{\boldsymbol{h}} \cdot \boldsymbol{S} + \hat{H}_0 + \hat{H}_{\mathrm{env}}[\hat{\boldsymbol{h}}] \tag{8.1}$$

Where $\hat{\boldsymbol{h}}$ describes the environmental degrees of freedom coupled with the impurity and $\hat{H}_0$ describes the impurity within the total quantum system.

The goal to understand the thermodynamics and dynamics of quantum impurity models led to the development of many ground-breaking numerical methods such as renormalization group methods [11], functional integral techniques for in-and-out of equilibrium [22] and many more. However, a striking difficulty regarding both analytical and numerical calculation occurs due to the interaction term in the Hamiltonian, as its general form consists of the Feynmann-Vernon functional integral.

Common approaches to circumvent this functional term are to employ Markovian approximations or Zero Order Functional Estimation (ZOFE) in the case of NMQSD. HOPS however provides another ansatz to obtain exact, non-markovian stochastic numerical solutions.

Numerical results are shown for the bosonic impurity models, however, the purpose of the fermionic impurity models is to explore and set up the motivation to implement the HOGTPS in the future, continuing from this thesis.

8.1 Bosonic Impurity Models

Considering an impurity and bath that follows bosonic statistics, the spin-boson model is one of the central paradigms. The quantum mechanical two-state system (spin 1/2 or qubit) interacting with a bosonic bath is the simplest model to describe the effect of an environment on constructive and destructive interference [17]. Its comprehensive investigation of decoherence and damping on quantum systems results in numerous applications ranging from electron transfer to quantum information processing [20].

The characteristics of the harmonic bath in contact with the two-state system are captured by the spectral density function of the bath [2]. A special case in the spin-boson model is considering an ohmic spectral density. This implies that the impurity is damped equally at all frequencies [2].

The respective Hamiltonian for this model is given by:

$$\tilde{H} = -\frac{\hbar\Delta_0}{2}\sigma_x - \frac{\hbar\varepsilon}{2}\sigma_z + \frac{1}{2}\sigma_z\hbar\sum_k \tilde{\lambda}_k\left(\tilde{b}_k^\dagger + \tilde{b}_k\right) + \sum_k \hbar\tilde{\omega}_k\tilde{b}_k^+\tilde{b}_k \tag{8.2}$$

Where $\tilde{\mathrm{b}}_\mathrm{k}^\dagger$ and $\tilde{b}_k$ are the creation and annihilation operators of the k-th bath mode with frequency $\tilde{\omega}_\mathrm{k}$. The Spin-Boson model, like the quantum impurity model consists of three parts. The impurity, the environment and the interaction between the two.

The first term in (8.2) describes the two-state system; a spin1/2 impurity, which can be tuned via the tunnelling parameter Δ and the additional bias ϵ. σ_x and σ_z represent Pauli Matrices. The second term in (8.2) represents a non-charged, non-interacting environment which is characterized by non-interacting harmonic oscillators with frequencies ω_i. The corresponding occupation numbers are given by the standard operator $\mathrm{n_i} = \tilde{\mathrm{b}}_\mathrm{k}^\dagger \cdot \tilde{\mathrm{b}}_\mathrm{k}$. The final term in the (8.2) corresponds to the interaction term. The z-th component of the spin couples linearly to each oscillator mode with λ_i specifying the coupling strength.

The spectral density of the bath nodes is assumed to have a Lorentzian peak at the characteristic frequency Ω but behaves Ohmically at low frequencies with a coupling strength $\alpha = \frac{\mathrm{J}(\omega)}{\omega}$. The Ohmic spectral density is formulated as:

$$J_{\mathrm{Ohm}}(\omega) = \sum \nu_k^2\Delta\left(\omega - \omega_k\right) = \kappa\omega e^{-\omega/\omega_c} \tag{8.3}$$

Where ω_c is a cut-off frequency. κ is a dimensionless parameter describing the coupling strength between the impurity (spins) and the bosons in the bath. The exponent in the spectral density function characterizes the distribution of the bath modes. There are three different regions for this exponent which lead to different properties of the model: the super-ohmic case ($\frac{\omega}{\omega_\mathrm{c}} > 1$), the ohmic case ($\frac{\omega}{\omega_\mathrm{c}} = 1$) and the sub-ohmic case ($\frac{\omega}{\omega_\mathrm{c}} < 1$).

The coupling term κ shows profound significance towards characterizing the model as it aids in explaining the phases and the respective phase transition within the model, making it the ordered parameter according the Landau's theory. The two phases exhibited by the spin-boson model are the delocalized phase and the localized phase. The delocalized phase describes a tunnelling between the σ_z eigenstates outweighs the coupling in the z-direction leading to a weak coupling phase. This results in the ground state consisting of a superposition of spins directed in the up and down direction leading to a vanishing magnetization in the coupling direction ($\sigma_\mathrm{z} = 0$). The localized phase is the strong coupling phase, where the spins are localized in the direction of bath coupling leading to a two-fold degenerate ground state with finite magnetization.

At zero temperature, a quantum phase transition can occur between the localized and the delocalized phase which is controlled by the coupling parameter. In the super-ohmic case, no phase transition occurs as the spin is always delocalized and no average magnetization is present. In the ohmic case, both localized and delocalized phases are present and the system undergoes a Kosterliz-Thouless transition in

1-D [22]. In a sub-ohmic bath, a second-order quantum phase transition between the localized phase and the delocalized phase takes place.

Equation (8.2) characterized by equation (8.3), cannot be generally solved explicitly as of its infinite dimension. Even suitable truncations of each harmonic oscillator do not solve this problem. However, since the original motivation is to model the dynamics of the system part including dissipation, the main task should be to calculate the non-unitary dynamics of the reduced density matrix:

$$\rho_{\mathrm{sys}}(\mathrm{t}) = \mathrm{Tr}_{\mathrm{env}}\rho(\mathrm{t}) \tag{8.4}$$

Where the total state $\rho(\mathrm{t})$ evolves unitarily according to the Von-Neumann equation $\mathrm{i}\dot{\rho}(\mathrm{t}) = [\mathrm{H}, \rho(\mathrm{t})]$ and $\mathrm{Tr}_{\mathrm{env}}$ denotes the partial trace over the environmental modes. under suitable conditions, the reduced dynamics can be calculated efficiently in a perturbative manner using time-local master equations. However, when leaving the perturbative regime the calculation of the reduced dynamics becomes substantially more challenging.

8.1.1 Realization of Spin-Boson Models

Platforms for quantum simulations are a test bed for many theoretical predictions for many-body physics. Engineering these platforms requires extreme precision and control of the system to replicate the nature of such a system established by the theory, for example, if a canonical ensemble is used or if the particle statistics are fermionic or bosonic. Engineering such a protocol would be efficient if it is supported by numerics predicting how such a platform would exhibit properties of the theoretical model (dissipative dynamics, phase transitions, etc.)

A one-dimensional transmission line can be used to engineer the required ohmic resistance. A one-dimensional transmission line is understood as an ensemble of harmonic oscillators with a fixed cutoff frequency [23].To give a brief overview of how different platforms could be used to realize a spin-boson model, some examples (which are explored more in detail later) are:

1. Superconducting transmission lines shown in figure (8.1a):
    - With charge qubits built out of Cooper pair superconducting boxes coupled to transmission lines, the dissipative spin-boson model can be realized.
    - The charge Qubit can be seen as a spin-1/2 particle that corresponds to the two degenerate charge states.
    - The gate voltages of the transmission lines act similarly to an effective magnetic in the spin-boson model as it can control the two charge states.
    - Placing the gate-source in series with an external resister describes a spin-boson model with ohmic dissipation [23].
2. Ultra-cold atoms shown in figure (8.1b):
    - Spin-1/2 particles can be engineered with one atom in a tight optical trap limit [24].
    - Bath modes refers to sound modes of a 1-D Bose-Einstein condensate [24]
    - Coupling between the bath and the optical trap is mediated through optical Raman transitions and collisional interactions [25]

Both cases here describe a situation with Ohmic dissipation, which is important as it allows for easy implementation of the HOMPs algorithm. The main reason is that the bath correlation function has a simple form which eases the hindrances on the numerical stability while performing HOMPs. Several other platforms have also been realised experimentally for the spin-boson model, advancing the field of quantum simulations. A few examples of different platforms are circuit-QED arrays [26] and edge states of quantum Hall systems [27].

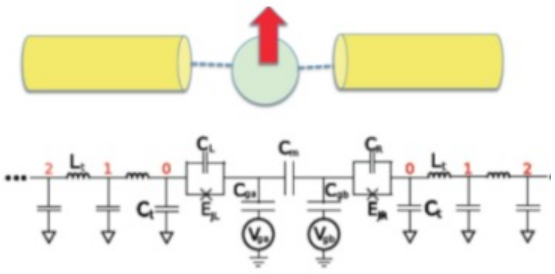

(a) An array of Josephson Junctions in series to gain an ohmic dissipation of the spin-boson model [23].

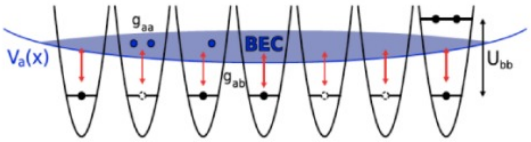

(b) Cold-atom setup that can either host one or no particle of an arbitrary atomic species b with one-site interactions U_{bb} that describes the spins. Which are coupled to a BEC through scattering g_{ab} and Raman coupling (red arrows) to another atomic species a confined to trapping potential $V_a(x)$ [24]

Figure 8.1 Spin-boson engineering. Realizing the spin-boson model with ohmic dissipation in superconducting circuits (a) and cold-atoms (b)

Spin-Boson Model

The Hamiltonian for a spin-boson model in a thermal bath is similar to the Hamiltonian in equation (8.2). As the engineered platforms of ultra-cold atoms and Josephson junctions are in the low temperature and high damping limits, this will be also considered in the simulation for the spin-boson model in a thermal bath. Using the Hierarchy of Matrix Product States, the dissipative dynamics for such a model can be numerically approximated and is shown in figure (8.2). The MPO for the effective stochastic representation of the spin-boson Hamiltonian (8.2) is given in equation (8.5).

$$\boldsymbol{W}^{[1]\prime} := \begin{pmatrix} -i\mathbb{I} & i(\frac{1}{2}\cdot\sigma_z\bar{\lambda_k}) & i(\frac{1}{2}\cdot\sigma_z\bar{\lambda_k})^\dagger & -\frac{\hbar\Delta_0}{2}\sigma_x - \frac{\hbar\varepsilon}{2}\sigma_z + i\hat{z}_t^*\sigma_z \\ 0 & 0 & 0 & 0 \\ 0 & 0 & 0 & 0 \\ 0 & 0 & 0 & 0 \end{pmatrix},$$

$$\boldsymbol{W}^{[k+1]\prime} := \begin{pmatrix} \mathbb{I} & 0 & 0 & \omega_k\hat{N}_k \\ 0 & \mathbb{I} & 0 & \frac{-d_k}{\sqrt{|d_k|}}b_k'^\dagger \\ 0 & 0 & \mathbb{I} & \sqrt{|d_k|}\hat{b}_k' \\ 0 & 0 & 0 & \mathbb{I} \end{pmatrix}, \quad k = 1, 2, \ldots, K, \tag{8.5}$$

In the spin-boson model, the system Hamiltonian is defined as $\bar{H}_s = -\frac{\hbar\Delta_0}{2}\sigma_x - \frac{\hbar\varepsilon}{2}\sigma_z$ and the interaction operator $\hat{L}$ is given by σ_z.The noise generation $\hat{z}_t^*$ for the bosonic bath is generated by the stochastic Gaussian noise. In the following tensor network simulations, $N = 2000$ realizations were used with a truncation of hierarchy order $N_{trunc} = 10$ and a maximum bond dimension of $\chi_{max} = 10$

Spin-Boson in Ladder Systems

Originally proposed by [25], a spin-boson model can be realized using ultra-cold atoms. First consider the system defined on a ladder geometry, which is the low energy excitations of a two-legged bosonic ladder [25]. In [22], the researchers propose that such a ladder geometry on a lattice where the spin-1/2 is used to probe a Mott-Superfluid transition. Such a setup consisting of a ladder geometry is illustrated in figure (8.3). The interaction between the double-well system (U_s) has to be sufficiently strong such that a state with one atom on the two wells is realized. The rest of the ladder forms the environment(bath). Since the two locations of the double-well potential correspond to the two different polarization states of a spin-1/2 particle, a particle can hop to and from the impurity with the amplitude $t_{\parallel,s}$, which the hopping

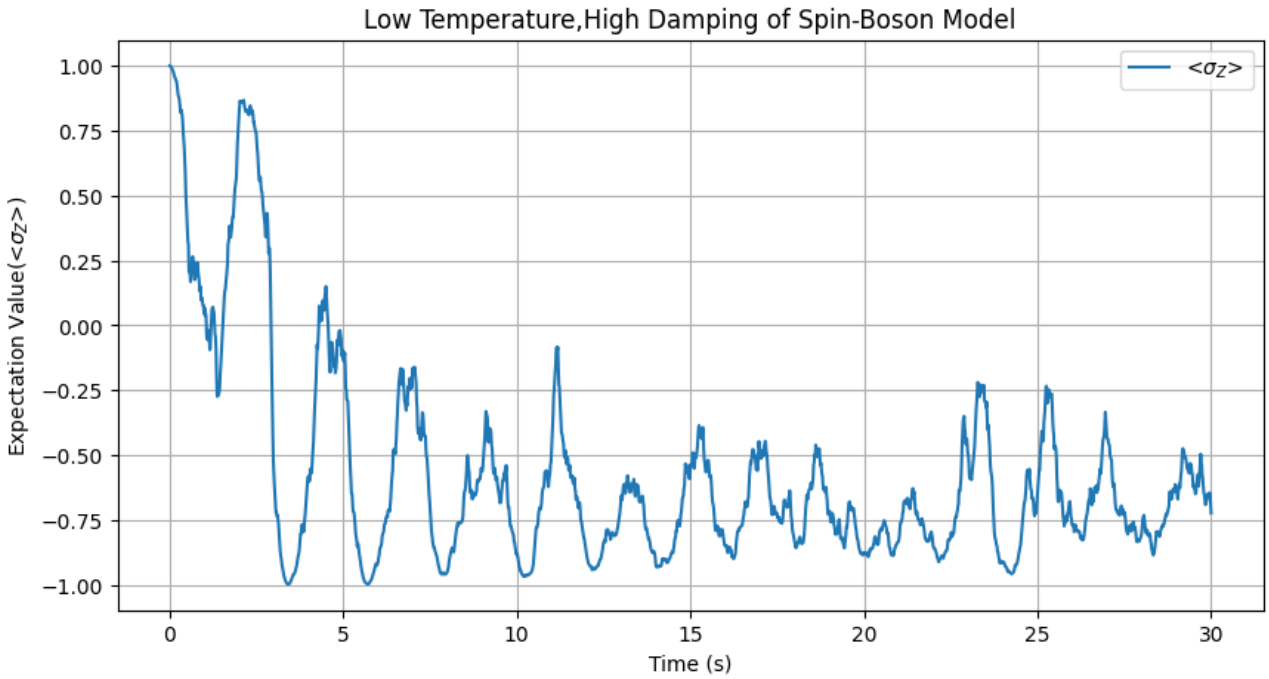

Figure 8.2 Dissipative Dynamics of a Spin-Boson model in a highly damped regime in the presence of a low-temperature thermal bath. $N = 2000$ realizations, $N_{trunc} = 10$ and bond dimension $\xi = 10$ were used for this HOMPS simulatio

amplitude of the particle exchange between the spin and the bath respectively. The Hamiltonian is defined as:

$$\begin{aligned} \hat{H} &= \sum_q \nu|q| b^\dagger_{a,q} b_{a,q} + \frac{\sigma_z}{2} \sum_{q\neq 0} \lambda_q \left(b^\dagger_{a,q} + b_{a,-q} \right) + (nV_x + \Delta_0)\sigma_x \\ \lambda_q &= \nu \sqrt{\frac{\pi|q|}{L}} \left(\frac{aV_z}{2\pi\nu} \sqrt{K} - \frac{1}{\sqrt{K}} \right). \end{aligned} \tag{8.6}$$

The parameters in equation (8.6) are defined in the table below:

a	$b_{a,q}$	Δ_0	L	n	U	v	K
Lattice Spacing	Bosonic mode coupled to Impurity mode	Direct Tunnel Coupling	Total Length of the ladder	Filling of the bath	one-site Bose-Hubbard interactions	speed of sound associated to the symmetric mode of bath	Luttinger parameter

The speed of sound associated with the mode of the bath and the Luttinger parameter are defined as [28]:

$$\nu = a\sqrt{2nt_\parallel U}, \quad K = 2\pi\sqrt{\frac{nt_\parallel}{2U}} \tag{8.7}$$

Where $t_\parallel$ are amplitudes of hopping between different sites in the bath. To finally identify an ohmic spin-boson model, coupling amplitudes V_z and V_X have to be defined as:

$$\begin{aligned} V_z &= -t^2_{\parallel,s} \left(\frac{1}{\mu + Un} - \frac{1}{V_{\perp,s} - \mu} + \frac{1}{U_s - \mu} \right), \\ V_x &= -t^2_{\parallel,s} \left(\frac{1}{\mu + Un} - \frac{1}{V_{\perp,s} - \mu} \right). \end{aligned} \tag{8.8}$$

Where μ is the chemical potential and $V_{\perp,s}$ is the on-site interaction terms for the Bath. A dimensionless parameter α which can identify the which dissipative regime the model is in (damped, underdamped, critical) for a Hamiltonian (8.6) is defined as:

$$\alpha = \frac{1}{2K} \left(\frac{V_x}{2U} - 1 \right)^2 \tag{8.9}$$

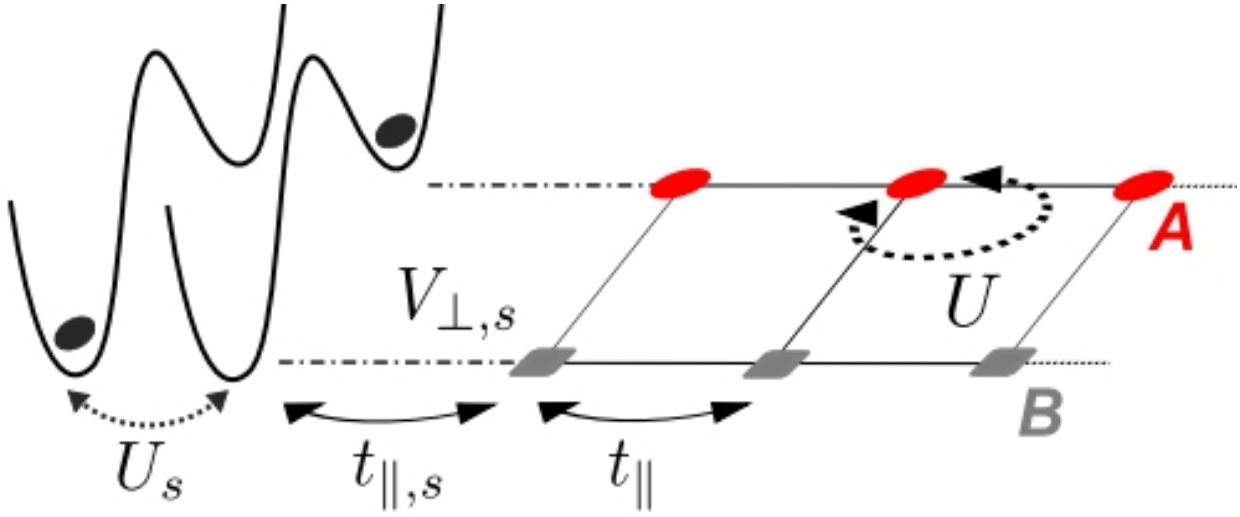

Figure 8.3 Model of the spin-impurity coupled to the low-energy excitations of the two-leg bosonic ladder [22]

These different regimes can be seen in the phase diagram of this model. In [22], by fixing the chemical potential in the ladder, the mean density is fixed $n = 1$. A Kosterlitz-Thouless type transition is observed in the phase diagram [28]. When α is zero, the phonons become suppressed due to charge quantization and the Luttinger parameter of the bath is renormalized to zero, resulting in the complete decoupling of the spin from the bath. When $\alpha < \frac{1}{2}$, the Rabi oscillations are in the underdamped regime and when $\alpha > \frac{1}{2}$ the system is in the overdamped regime [29].

Using the finite-state machine algorithm [14], the MPO for the ladder spin-boson model is given by:

$$\boldsymbol{W}^{[1]\prime} := \begin{pmatrix} -i\mathbb{I} & i(\frac{1}{2}\cdot\sigma_z\bar{\lambda_k}) & i(\frac{1}{2}\cdot\sigma_z\bar{\lambda_k})^\dagger & (nV_x+\Delta_0)\sigma_x + i\hat{z}_t^*(\frac{1}{2}\cdot\sigma_z\bar{\lambda_k}) \\ 0 & 0 & 0 & 0 \\ 0 & 0 & 0 & 0 \\ 0 & 0 & 0 & 0 \end{pmatrix},$$

$$\boldsymbol{W}^{[k+1]\prime} := \begin{pmatrix} \mathbb{I} & 0 & 0 & \omega_k\hat{N}_k \\ 0 & \mathbb{I} & 0 & \frac{-d_k}{\sqrt{|d_k|}}b_k'^\dagger \\ 0 & 0 & \mathbb{I} & \sqrt{|d_k|}\hat{b}_k' \\ 0 & 0 & 0 & \mathbb{I} \end{pmatrix}, \quad k = 1, 2, \ldots, K, \tag{8.10}$$

In MPO (8.10), the interacting parameter $\bar{\lambda_k}$ is given by equation (8.6), which encodes the information about the coupling amplitudes of the double-well, speed of sound in the bath mode and the Luttinger parameter which all characterize the ultra-cold experiment. Using the values for the parameters in equation (8.6) found in [22], the dissipative dynamics for such an operator can be simulated using HOMPS (8.10). The results are shown in figure 8.4. The Rabi oscillations can be seen in figure (8.4) and are similar to the oscillations shown in figure (8.4). Since [22] only considers the coherent regime of the dissipative parameter (8.9), such Rabi oscillations are expected. Therefore, the platform for such a ladder geometry using ultra-cold atoms with appropriate system settings (Luttinger parameter, tunnelling values, etc.) could be ideally used to an extent to simulate the spin-boson model experimentally. This numerical simulation does not take into account several other experimental parameters which could directly influence the dynamics of the spins within such a system, therefore, this result does not completely justify using ultra-cold atoms, although from a numerical standpoint, the arguments are supported and are in agreement [25]. The Hamiltonian (8.6) is shown to be in agreement regardless with the spin-boson model [25].

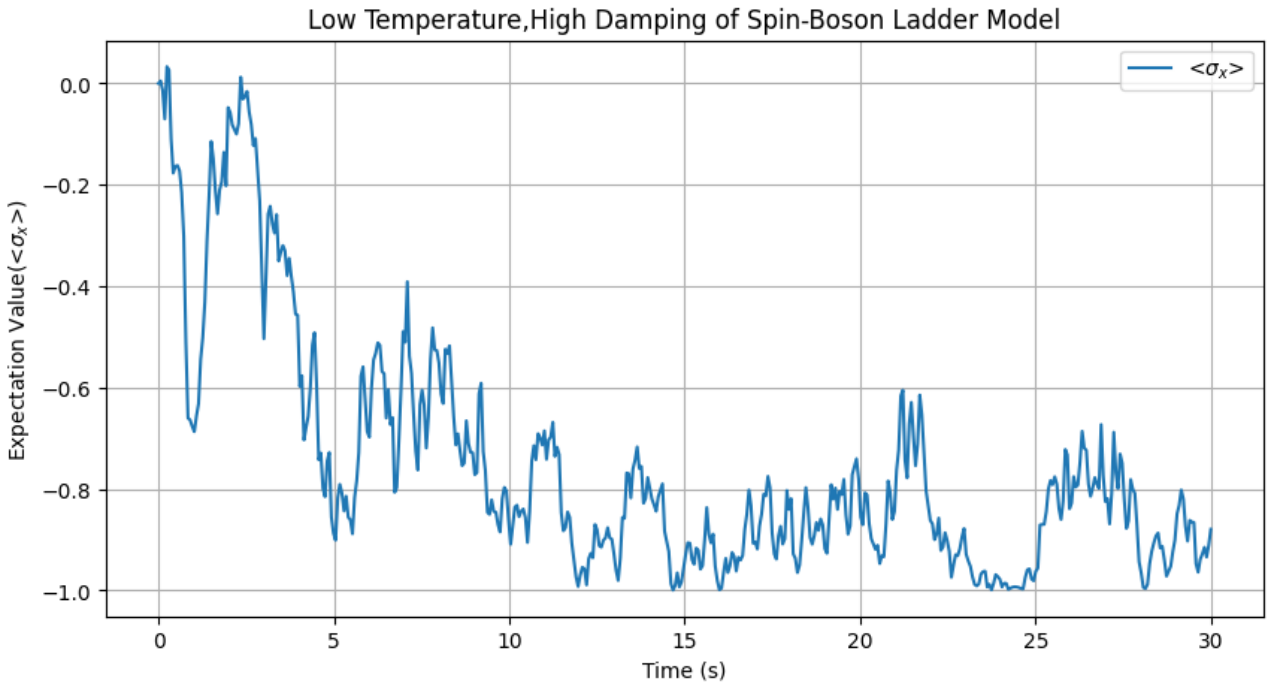

Figure 8.4 Dissipative dynamics of a spin-boson model simulated using an engineered Hamiltonian ultra-cold atoms in a ladder geometry within the high damping regime and low temperature. $N = 2000$ realizations, $N_{trunc} = 10$ and bond dimension $\xi = 10$ were used for this HOMPS simulation

Realizing Spin-Boson model in Josephson Circuit

Developing from the ladder geometry spin-boson model discussed in the previous section, a similar geometry can be understood for superconducting systems intuitively by considering a two-level system which corresponds to two charged states on such a system [23]. Summarizing the idea proposed by [23], the states in a superconductor can be modelled by harmonic oscillators by describing the quantum excitations in two long transmission lines as Harmonic oscillators. An illustration is given in Such a model can be energetically described through the Hamiltonian at half-filling (8.11) [30]:

$$\hat{H} = \sum_{k>0} \nu_a |k| \left(b_{ak}^{\dagger} b_{ak} + \frac{1}{2} \right) - \frac{h_x}{2} \sigma_x - \frac{E_J}{2} \sigma_x - \sum_{k>0} \lambda_k (b_{ak} + b_{ak}^{\dagger}) \frac{\sigma_x}{2} \tag{8.11}$$

The symmetric ladder operators b_{ak} in (8.11) are combinations of the operators (b_{lk} and b_{rk}) that create/destroy an excitation in mode k in the left and right transmission lines. The effective tunnelling of Cooper pairs from the left to right transmission lines is characterized by an effective Josephson coupling E_J (which is analogous to the spin-boson model as the transverse parameter Δ_0 in equation (8.2)). To characterize the different dissipative regimes for the Hamiltonian (8.11), the dissipative parameter α [22]:

$$\alpha = \frac{2R}{R_Q} (\gamma_l^2 + \gamma_r^2) \tag{8.12}$$

In equation (8.12), R_Q is the quantum resistance given by $\frac{2\pi}{(2e)^2}$ for a Cooper pair charge of $2e$, R is the internal resistance of each transmission line and finally, $_l$ and γ_r are the effective dimensionless couplings of the qubit on the left and right transmission lines respectively. The different damping regimes are characterized by the same values for α as in the ultra-cold atom model (8.6).
To perform the HOMPS simulation, the effective stochastic Hamiltonian has to be defined. Following the

similar approach in the last two subsections, we first define an MPO using the finite-state machine algorithm [14]. The MPO is defined in equation (8.13).

$$\boldsymbol{W}^{[1]\prime} := \begin{pmatrix} -i\mathbb{I} & i\left(\frac{1}{2}\lambda_k\sigma_x\right) & i\left(\frac{1}{2}\lambda_k\sigma_x\right)^\dagger & -\frac{h_x}{2}\sigma_x - \frac{E_J}{2}\sigma_x + i\hat{z}_t^*\left(\frac{1}{2}\lambda_k\sigma_x\right) \\ 0 & 0 & 0 & 0 \\ 0 & 0 & 0 & 0 \\ 0 & 0 & 0 & 0 \end{pmatrix},$$

$$\boldsymbol{W}^{[k+1]\prime} := \begin{pmatrix} \mathbb{I} & 0 & 0 & \omega_k\hat{N}_k \\ 0 & \mathbb{I} & 0 & \frac{-d_k}{\sqrt{|d_k|}}\nu_a|k|b_k'^\dagger \\ 0 & 0 & \mathbb{I} & \sqrt{|d_k|}\nu_a|k|\hat{b}_k' \\ 0 & 0 & 0 & \mathbb{I} \end{pmatrix}, \quad k = 1, 2, \ldots, K, \tag{8.13}$$

Since in the Hamiltonian for the Josephson circuit (8.11), the system Hamiltonian is defined as $\hat{H}_s = -\frac{h_x}{2}\sigma_x - \frac{E_J}{2}\sigma_x$ and the exchange operator is $\hat{L} = \frac{1}{2}\lambda_k\sigma_z$. With the MPO in (8.13) and the parameter values for the effective Josephson coupling E_J, the dimensionless coupling between the qubits γ_l and γ_l, and the dissipative parameter in equation (8.12) is given taken directly from [22], the HOMPS simulation can be performed. The results from are shown in figure (8.5) The first few seconds in figure (8.5) display the

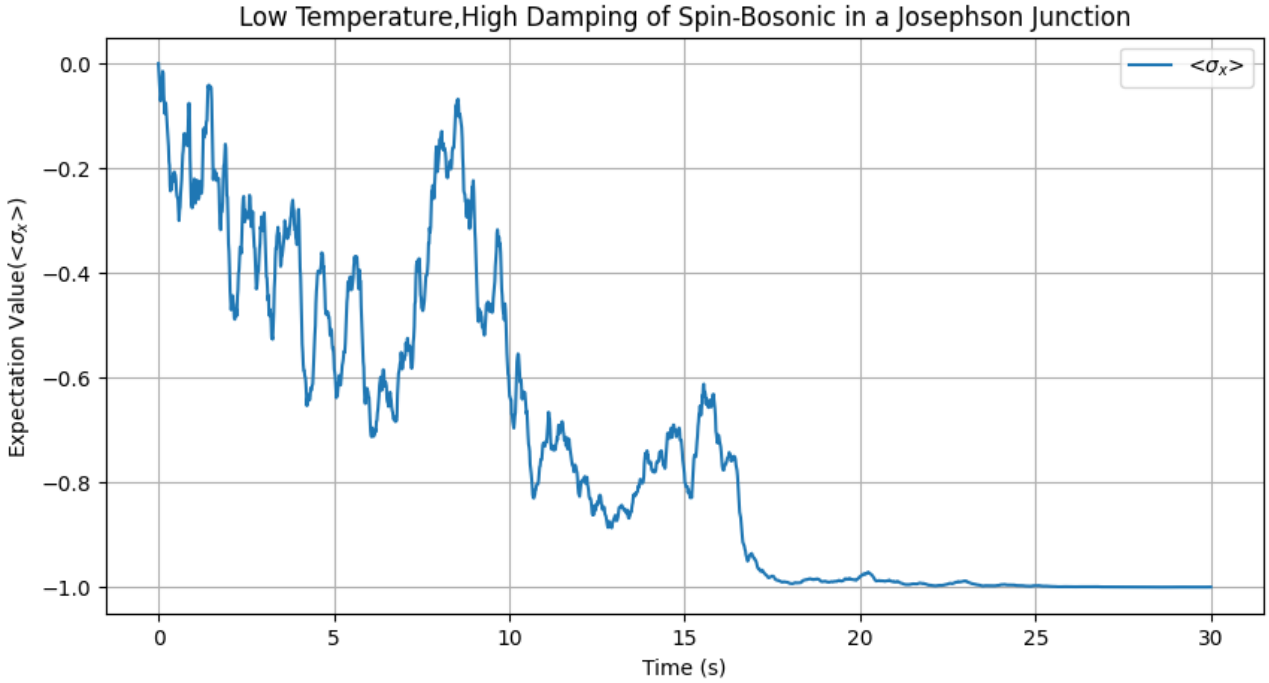

Figure 8.5 Dissipative dynamics of a spin-boson model simulated using an engineered Hamiltonian consisting of superconducting Josephson Junctionsin a ladder geometry within the high damping regime and low temperature. N = 2000 realizations, Ntrunc = 10 and bond dimension = 10 were used for this HOMPS simulation

Rabi oscillations which are expected for a spin-boson model, however, after $t = 5$ seconds the numerical results appear to be unstable. This could be due not properly choosing the bond dimension in the HOMPS tensor network, or instabilities that arised from including the values for the parameters in the engineered Josephson junction Hamiltonian (8.11) gained from [22].

8.2 Fermionic Impurity Models

Preliminary research was done regarding the physics of fermionic impurity models. Although no numerical results are available to be shown, the theory supporting these models is presented in this section along with a derived Ansatz for how the HOGTPS method for the one-qubit in a fermionic environment case.

The study of Fermionic impurity models has a lot of attention due to its applications in quantum optical systems, As these systems comprise one or multiple few-level quantum systems coupled to a dissipative environment [31]. Especially in modern quantum technologies, particular interest in systems of quantum emitters in structured baths (environments with non-trivial spectral properties) [32].

Coupling a single excited emitter to a bath with a gapped band structure can lead to fractional decay due to population trapping in an emitter-bath bound state [33]. Such bound states can mediate purely coherent long-range interactions between multiple emitters, enabling the diverse simulation of quantum many-body models [32]. These structured baths also give rise to a variety of novel dissipative phenomena, such as chiral emission dynamics and non-exponential decay [33].

In condensed matter theory, fermionic impurity models play a significant role in a variety of systems, an example of this is individual localised fermionic impurity levels can affect transport properties in mesoscopic systems [31], and their presence in superconductors can lead to the emergence of localised quasiparticle states or Majorana modes [31]. Recent proposals of cold-atom matter-wave analogues to traditional waveguide QED setups provide a quite natural pathway to explore these models from a quantum optics perspective [31]

The free-fermion formalism will be considered in this section. Fermionic impurities are described by creation and annihilation operators $\tilde{\mathrm{c}}_{\mathrm{k}}^{\dagger}$ and $\tilde{c}_k$ which follow anti-commutation relations (CAR). These impurities are coupled via local tunnelling to a d-dimensional spinless fermionic bath of $\mathrm{L}^{(}\mathrm{d}$ sites. The bath modes are therefore described as operators $\left\{\mathrm{b}_{\mathrm{j}}^{\dagger}, \mathrm{b}_{\mathrm{j}}\right\}_{\mathrm{j}=1}^{\mathrm{L}^{\mathrm{d}}}$.

The respective Hamiltonian is defined as:

$$\begin{aligned} H_S &= \Delta \sum_n c_n^{\dagger} c_n \\ H_B &= 2^d J \sum_j b_j^{\dagger} b_j - J \sum_{\langle j,j' \rangle} \left(b_j^{\dagger} b_{j'} + \text{ H.c. } \right), \\ V &= g \sum_n \left(c_n^{\dagger} b_{j_n} + \text{ H.c. } \right). \end{aligned} \tag{8.14}$$

Where $\mathrm{H_S}$ represents the impurity subsystem, $\mathrm{H_B}$ is the bath Hamiltonian and V is the interaction Hamiltonian describing the coupling between the impurity and bath as in the bosonic case. The main difference here is that the impurity Hamiltonian and the bath Hamiltonian anti-commute with each other due to the presence of fermions. Setups considering commuting bath-impurity models have also been considered [33] but will not be focused upon in this thesis.

The bath Hamiltonian in (8.14) can be diagonalized using a Fourier transform since a property of the bath Hamiltonian is that it is translational-invariant and it has a single site per unit cell. This results in:

$$\begin{aligned} H_B &= \sum_{\boldsymbol{k}} \omega_{\boldsymbol{k}} b_{\boldsymbol{k}}^{\dagger} b_{\boldsymbol{k}} \\ V &= \frac{g}{\sqrt{L^d}} \sum_{n,\boldsymbol{k}} \left(e^{i\boldsymbol{k}\cdot\boldsymbol{r}_n} c_n^{\dagger} b_{\boldsymbol{k}} + \text{ H.c. } \right) \end{aligned} \tag{8.15}$$

Where the shorthand notation $\mathrm{r_n} = \mathrm{r_{i_n}}$ denotes the position of the j-th bath site.

The spectrum consists of a single band $\omega_k \in \left[0, 2^{d+1}J\right]$, and the one-site potential Δ constitutes a detuning for the lower band edge. The spectrum is modelled using the dispersion relation of 8.14 which is given as $\omega_{\mathrm{k}} = 2\mathrm{J}(1 - \cos(\mathrm{k})$ for d=1.

Since the Hamiltonian in (8.14) conserves the particle number, studying the dynamics produces a well-defined number of particles for a given initial state, allowing a restriction to a smaller subspace within the Hilbert space consisting of the same number of particles. While considering the thermodynamic limit, the Fermi-level or the filling fraction is defined in terms of the ground state of $\mathrm{H_B}$ with the highest energy of occupied bath eigenmodes. The ground state is given as:

$$|\mathrm{FS}\rangle = \left(\prod_{\omega_k < E_F} b_k^\dagger \right) |\mathrm{vac}\rangle \tag{8.16}$$

Where "FS" stands for the Fermi sea and "vac" denotes the vacuum state. A Fermi level less than or equal to zero identifies an empty bath, whereas a level greater than $2^{\mathrm{d}+1}\mathrm{J}$ corresponds to a fully occupied bath. By replacing the impurity and bath modes with spin and boson operators, the standard Hamiltonian employed in quantum optics to describe quantum emitters coupled to structures (photonic) environments is recovered from equation (8.14).

Implementing the Free-Fermion formalism is non-trivial in this context as the Hamiltonian described in (8.14) is quadratic in fermionic operators, reflecting the fact that the fermions are non-interacting.

Considering M independent fermionic creation and annihilation operators $\{\psi_l^\dagger, \psi_l\}_{l=1}^M$. Assuming a complete set, the states $\{|\psi_l\rangle = \psi_l^\dagger |\mathrm{vac}\rangle\}_{l=1}^M$ form an orthonormal basis of the single-particle Hilbert space. A basis of the whole many-body Hilbert space is then given by the Fock states: $|\boldsymbol{n}\rangle \equiv \left(\psi_1^\dagger\right)^{n_1} \dots \left(\psi_M^\dagger\right)^{n_M} |\mathrm{vac}\rangle$ where the state can be either 0 or 1 due to Pauli's exclusion principle. For an arbitrary quadratic operator $O = \sum_{l,m} O_{lm} \psi_l^\dagger \psi_m$, the expectation value can be expressed as:

$$\begin{aligned} \langle \boldsymbol{n}' | \, O \, | \boldsymbol{n} \rangle = \sum_{l,m} & O_{lm} n'_l n_m \Delta_{\boldsymbol{n}' - \boldsymbol{e}^l, \boldsymbol{n}\boldsymbol{e}^m} \\ & \times (-1)^{\sum_{j<l} n'_j + \sum_{j<m} n_j} \end{aligned} \tag{8.17}$$

The expectation value in (8.17) is non-vanishing only if the bra and ket have the same number of particles and differ at most by one pair of occupation numbers, meaning only diagonal elements are non-vanishing. The single-particle eigenmodes $\{\phi_l^\dagger, \phi_l\}_{l=1}^M$ as they diagonlize the Hamiltonian as $H = \sum_l \varepsilon_l \phi_l^\dagger \phi_l$. With this, the ground state for a given Fermi level is:

$$|\mathrm{GS}\rangle = \left(\prod_{\varepsilon_l < E_F} \phi_l^\dagger \right) |\mathrm{vac}\rangle \tag{8.18}$$

Since the Hamiltonian (8.14) is quadratic, a further conclusion that can be made is that it is linked with the theory of Gaussian states, since Gaussianity is preserved under the evolution with a quadratic Hamiltonian [32]. A property of Gaussian states is the fact that any even-ordered correlations can be expressed entirely in terms of 2-point correlations according to Wick's theorem. Therefore, Gaussian states are characterised fully by their covariance matrix [32]. This is important as this characteristic allows for the stochastic description of the evolution of the wave equation in (8.14).

For a non-Markovian stochastic equation for an open system coupled to a fermionic bath, in the interaction picture, the Hamiltonian is [34]:

$$\hat{H}_{\mathrm{tot}}(t) = \hat{H}_{\mathrm{s}} + \sum_i (g_i^* e^{i\omega_i t} \hat{c}_i^\dagger \hat{L} + g_i e^{-i\omega_i t} \hat{L}^\dagger \hat{c}_i) \tag{8.19}$$

Where $\hat{H}_s$ is the system Hamiltonian, $\hat{H_B}$: is the bath Hamiltonian (consisting of fermions) and $\hat{H_{int}}$ is the interaction Hamiltonian. The FHOPS representation in equation (3.17) can be gained from (**??**). Furthermore, the effective stochastic Hamiltonian can be defined as

$$\begin{aligned} \hat{H}_{\mathbf{b}} &= \sum_i \omega_i \hat{c}_i^\dagger \hat{c}_i, \\ \hat{H}_{\mathrm{int}} &= \sum_i (g_i^* \hat{c}_i^\dagger \hat{L} + g_i \hat{L}^\dagger \hat{c}_i), \end{aligned} \tag{8.20}$$

To apply the HOGTPS Ansatz, the effective stochastic Hamiltonian must be defined from the Hamiltonian (8.14).

From this short introduction to Fermionic impurity models, it can be seen that the tools mentioned and developed in the previous sections can be easily applied within this context. We first start by writing the total Hamiltonian in equation (8.14) as a stochastic Hamiltonian by introducing the Grassmannian noise process (as the bath consists of fermions). The effective stochastic Hamiltonian can be written as analogously to equation (7.2). A toy model will be first considered before moving to the Kondo Model.

8.2.1 One-Qubit Dissipative Model

As the title suggests, the toy model consists of a qubit (system) in a fermionic bath. The total Hamiltonian for the one-qubit dissipative model is defined as [34]:

$$\begin{aligned} \hat{H}_{\mathrm{tot}} &= \hat{H}_{\mathrm{s}} + \hat{H}_{\mathrm{b}} + \hat{H}_{\mathrm{int}}, \\ \hat{H}_{\mathrm{s}} &= \frac{\omega}{2} \hat{\sigma}_z, \\ \hat{H}_{\mathrm{b}} &= \sum_i \omega_i \hat{c}_i^\dagger \hat{c}_i, \\ \hat{H}_{\mathrm{int}} &= \sum_i (g_i^* \hat{c}_i^\dagger \hat{L} + g_i \hat{L}^\dagger \hat{c}_i), \end{aligned} \tag{8.21}$$

Where $\hat{L} = \hat{\sigma}_-$. The effective fermionic stochastic Hamiltonian is defined as:

$$\begin{aligned} \hat{H}_{\mathrm{eff}} =& \frac{\omega}{2} \hat{\sigma}_z + \hat{\sigma}_- \cdot \sum_i \frac{\partial}{\partial \eta_k} e^{i\omega_i t - i \sum_{k=1}^K \omega_k \hat{c}_k^\dagger \hat{c}_k} \\ & - i \hat{\sigma}_-^\dagger \sum_{k=1}^K \sqrt{|d_k|} \hat{c}_k + i \hat{\sigma}_- \sum_{k=1}^K \frac{d_k}{\sqrt{|d_k|}} \hat{c}_k^\dagger \end{aligned} \tag{8.22}$$

Where θ is a Grassmann generator. Using the correspondence in equation (2.20), the effective Hamiltonian in (8.22) can be expressed in terms of a Grassmann algebra:

$$\hat{H}_{\mathrm{eff}} = \frac{\omega}{2} \hat{\sigma}_z + i \hat{\sigma}_- \cdot Z_t^* - i \sum_{k=1}^K \nu_k \eta_k \frac{\partial}{\partial \eta_k} - i (\hat{\sigma}_-)^\dagger \sum_{k=1}^K \sqrt{|d_k|} \frac{\partial}{\partial \eta_k} + i \hat{\sigma}_- \sum_{k=1}^K \frac{d_k}{\sqrt{|d_k|}} \eta_k \tag{8.23}$$

Coding this symbolically in terms of [η,$\bar{\eta}$] and using GrassmannTN to obtain the matrix representation of (8.23), the finite-state machine algorithm can be applied to obtain a Grassmann tensor product state [14] as:

$$\boldsymbol{W}^{[1]\prime} := \begin{pmatrix} -i\mathbb{I} & i\hat{\sigma}_- & i\left((\hat{\sigma}_-)^\dagger\right) & \frac{\omega}{2}\hat{\sigma}_z + \sum_i e^{i\omega_i t}\partial/\partial\eta_i \cdot \hat{\sigma}_- \\ 0 & 0 & 0 & 0 \\ 0 & 0 & 0 & 0 \\ 0 & 0 & 0 & 0 \end{pmatrix},$$

$$\boldsymbol{W}^{[k+1]\prime} := \begin{pmatrix} \mathbb{I} & 0 & 0 & \omega_k \eta_k \frac{\partial}{\partial \eta_k} \\ 0 & \mathbb{I} & 0 & \frac{-d_k}{\sqrt{|d_k|}}\eta_k \\ 0 & 0 & \mathbb{I} & \sqrt{|d_k|}\frac{\partial}{\partial \eta_k} \\ 0 & 0 & 0 & \mathbb{I} \end{pmatrix}, \quad k = 1, 2, \ldots, K, \tag{8.24}$$

This was the initial setup for the GTPS, however, no numerical results were obtained due to timing constraints. The Kondo model and the Simple Impurity Anderson Model are included in Appendices A.3 and A.4 respectively.

9 Conclusion

This thesis explored the intersection between tensor network simulations of non-markovian dynamics and condensed matter theory. 1-D Impurity models consisting of a bosonic and fermionic bath were considered, with numerical results for bosonic impurity models whilst only a proposed approach for fermionic models was introduced. A non-markovian stochastic tensor network known as the Hierarchy of Matrix Product States was used to simulate the ohmic-dissipative dynamics of spin-boson models and their experimental realizations through ultra-cold atoms and Josephson circuits. The results for the dissipative dynamics are shown in figure (8.4) for the ultra-cold atoms while figure $(8.1a)$ shows the Josephson junction.

A new tensor network approach was introduced in this thesis to simulate spin-1/2 particles in a fermionic bath known as the Hierarchy of Grassmann Tensor Product States, which addressed the difficulty of simulating a Grassmannian stochastic noise. However, only the method and the MPO for this approach were derived, and numerical results benchmarking its performance is still an open question. For Fermionic impurity models, the HOGTPS approach was derived for a toy model of a qubit in a fermionic bath, other models such as the 1-D Simple Impurity Anderson Model and the Kondo model were mentioned as a model which could be explored to simulate such a tensor network algorithm.

For a future outlook, the first direction will be to implement the HOGTPS algorithm and to benchmark its performance extensively against other numerical methods to simulate open fermionic environments (Quantum Monte Carlo, Hierarchical Equations of Motion.). It will be interesting to further observe which type of fermionic models can be simulated and what factors about this approach affect the numerical results, such as the stability of the solution, the optimal bond dimension and the truncation of the hierarchy.

A Appendix

A.1 Derivation of Fermionic Hierarchy of Pure States

The order of functional derivative operators is important now since they anti-commute with each other. For the same reason, all auxiliary states with some $k_j > 1$ vanish as expected to follow the Pauli exclusion principle, as $D_{i,t}$ are linear combinations of fermionic annihilation operators. The functional integrals in (3.15) can be expressed as $\psi_t^{(1,0,\dots)} := D_{1,t}\psi_t, \quad \psi_t^{(0,1,\dots)} := D_{2,t}\psi_t, \quad \dots$, which allows for the following expression:

$$\partial_t \psi_t^{(0)} = -\mathrm{i}H\psi_t^{(0)} + \sum_j L_j Z_j^*(t)\psi_t^{(0)} - \sum_j L_j^\dagger \psi_t^{(e_j)} \tag{A.1}$$

An exponential form of the BCF is again assumed to obtain the equations of motion for the auxiliary states similar to the bosonic case. By taking the time derivative of ϕ_t^{k}:

$$\partial_t \psi_t^{(\boldsymbol{k})} = (\partial_t \boldsymbol{D}_t^{\boldsymbol{k}})\psi_t + \boldsymbol{D}_t^{\boldsymbol{k}}(\partial_t \psi_t) \tag{A.2}$$

Using that the second term on the right-hand side commutes with all the $D_{i,j}$, one obtains:

$$\partial_t \psi_t^{(\boldsymbol{k})} = -k\cdot\boldsymbol{w}\psi_t^{(\boldsymbol{k})} - \underbrace{\mathrm{i}H\psi_t^{(\boldsymbol{k})} + \sum L_j D_t^{\boldsymbol{k}} Z_j^*(t)\psi_t}_{*} - \underbrace{\sum L_j^\dagger D_t^{\boldsymbol{k}} D_{j,t}\psi_t}_{**} \tag{A.3}$$

$D_{j,t}$ must be ordered to obtain a closed equation for the auxiliary states. In (**) $D_{j,t}$ must be moved to the correct position due to the ordering of fermionic operators:

$$D_t^k D_{j,t} = (-1)^{k_J} D_{1,t}^{k_1}\dots D_{j,t} D_{J,t}^{k_J} = (-1)^{k_{j+1}+\dots+k_J} D_{1,t}^{k_1}\dots D_{j,t}^{k_j+1}\cdots D_{J,t}^{k_J}. \tag{A.4}$$

In (*), $Z_j^*(t)$ in front of D_t^K by using $\{D_{j,t}, Z_{j'}^*(s)\} = \delta_{jj'}\alpha(t-s)$ which results in:

$$\begin{aligned}
D_t^k Z_j^*(t) &= (-1)^{k_J} D_{1,t}^{k_1}\dots Z_j^*(t) D_{J,t}^{k_J} \\
&= (-1)^{k_{j+1}+\dots+k_J} D_{1,t}\dots D_{j,t}^{k_j} Z_j^*(t)\dots \\
&= (-1)^{|\boldsymbol{k}|_j} D_{1,t}\dots\left(-D_{j,t}^{k_j-1} Z_j^*(t) D_{j,t} + D_{j,t}^{k_j-1} g_j\right). \\
&= \dots\left(D_{j,t}^{k_j-2} Z_j^*(t) D_{j,t}^2 - D_{j,t}^{k_j-1} g_j + D_{j,t}^{k_j-1} g_j\right)\dots \\
&= \dots\left((-1)^{k_j} Z_j^*(t) D_{j,t}^{k_j} + (k_j \bmod 2) g_j D_{j,t}^{k_j-1}\right)\dots \\
&= (-1)^{|\boldsymbol{k}|} Z_j^*(t)\boldsymbol{D}_t^{\boldsymbol{k}} + (-1)^{|\boldsymbol{k}|_j}(k_j \bmod 2) g_j \boldsymbol{D}_t^{\boldsymbol{k}-\boldsymbol{e}_j}
\end{aligned} \tag{A.5}$$

Combining equations $(A.4)$ with $(A.5)$ results in an infinite hierarchy of pure states for a fermionic environment [2]:

$$\begin{aligned}
\partial_t \psi_t^{(\boldsymbol{k})} = &\left(-\mathrm{i}H - \boldsymbol{k}\cdot\boldsymbol{w} + (-1)^{|\boldsymbol{k}|}\sum_j Z_j^*(t) L_j\right)\psi_t^{(\boldsymbol{k})} \\
&+ \sum_j (-1)^{|\boldsymbol{k}|_j}(k_j \bmod 2) g_j L_j \psi_t^{(\boldsymbol{k}-\boldsymbol{e}_j)} \\
&- \sum_i (-1)^{|\boldsymbol{k}|_j}(-1)^{|\boldsymbol{k}|_j} L_j^\dagger \psi_t^{(\boldsymbol{k}+\boldsymbol{e}_j)}
\end{aligned} \tag{A.6}$$

As mentioned earlier, all states with a k_j value not equal to either zero or one vanish. This is ensured by the modulo term in $(A.6)$, therefore, states with some other k_j-values that are initially zero always remain zero which further means that the closed and finite hierarchy with all the appropriate k_j values results in a closed and finite hierarchy given as:

$$\begin{aligned}\partial_t \psi_t^{(\boldsymbol{k})} = &\left(-\mathrm{i}H - \boldsymbol{k}\cdot\boldsymbol{w} + (-1)^{|\boldsymbol{k}|}\sum_j Z_j^*(t)L_j\right)\psi_t^{(\boldsymbol{k})} \\ &+ \sum_j (-1)^{|\boldsymbol{k}|_j} g_j L_j \psi_t^{(\boldsymbol{k}-\boldsymbol{e}_j)} - \sum_j (-1)^{|\boldsymbol{k}|_j} L_j^\dagger \psi_t^{(\boldsymbol{k}+\boldsymbol{e}_j)}\end{aligned} \tag{A.7}$$

Which is the final expression for the HOPS for a fermionic environment.

It is immediately noticed that the finite system in $(A.7)$ consists of 2^J coupled equations (J is the number of modes), and a large number of modes J results in intractable large numerical simulations. Therefore, a useful truncation yields to be helpful through introducing a truncating order.

A.2 Norm of Grassmann Tensor Products

A simple example shown in [8], considers calculating the norm of the fermion occupation number $c^\dagger c$:

$$\begin{aligned}\langle\Psi|c_i^\dagger c_j^\dagger|\Psi\rangle &= \int \mathrm{d}\eta_i^*\mathrm{d}\eta_i(1-\eta_i^*\eta_i)\mathrm{d}\eta_j^*\mathrm{d}\eta_j(1-\eta_j^*\eta_j)\prod_{i'}\mathrm{d}\eta_{i'}^*\mathrm{d}\eta_{i'}(1-\eta_{i'}^*\eta_{i'})\eta_i^*\eta_j^*\Psi(\eta)\Psi(\eta^*) \\ &= -\sum_{a_M\bar{a}_M\ldots a_K\bar{a}_K\cdots\{m_{i'}\},\{a_{I'}\bar{a}_{I'}\}}\int \bar{T}^1_{j,\bar{a}_M\bar{a}_{N\cdots}}\bar{T}^1_{i,\bar{a}_K\bar{a}_{L\ldots}}\bar{G}_{ij;\bar{a}_I\bar{a}_J}T^0_{i;a_Ka_{L\ldots}}T^0_{j;a_Ma_{N\ldots}}G_{ij;a_Ia_J} \\ &\times\widetilde{\prod_{i'}}\bar{T}_{i';\bar{a}_{K'}\bar{a}_{L'}..}\prod_{i'j'}\bar{G}_{i'j';\bar{a}_{I'}\bar{a}_{J'}}\prod_{i'}T^{m_{i'}}_{i';a_{K'}a_{L'}..}\prod_{i'j'}G_{i'j';a_{I'}a_{J'}} \\ &= \sum_{\{a_{I'}\bar{a}_{I'}\}}\int T'_{i;a_K\bar{a}_K,a_L\bar{a}_{L\ldots}}T''_{j;a_M\bar{a}_M,a_N\bar{a}_{N\ldots}}G_{ij;a_I\bar{a}_I,a_J\bar{a}_J}\prod_{i'}T_{i';a_{K'}\bar{a}_{K'},a_{L'}\bar{a}_{L'\ldots}}\prod_{i'j'}G_{i'j';a_{I'}\bar{a}_{I'},a_{J'}\bar{a}_{J'}},\end{aligned} \tag{A.8}$$

Where T' and T'' are introduced as impurity tensors and are defined as:

$$T'_{i;a_K\bar{a}_K,a_L\bar{a}_{L\ldots}} = \bar{T}^1_{i;\bar{a}_K\bar{a}_{L\ldots}}T^0_{i;a_Ka_{L\ldots}}; T''_{j;a_M\bar{a}_M,a_N\bar{a}_{N\ldots}} = \bar{T}^1_{j;\bar{a}_M\bar{a}_{N\ldots}}T^0_{j;a_Ma_{N\ldots}}. \tag{A.9}$$

A.3 The Kondo Model

Focusing on an application of the fermionic impurity model, a classical example is the Kondo model. An experimental observation around the 1930s showed that the resistance in noble or divalent metals typically shows a minimum at low temperatures when containing small concentrations of transition metals [18]. It was theorised that the inelastic scattering is reduced with decreasing the temperature, therefore the resistance should also decrease linearly as a function of temperature, however, the experimental results showed that the increase of the residual resistance is proportional to the transition metal concentration [18] and only occurs when those impurities are magnetic. Kondo proposed a Hamiltonian which provides the physical picture explaining this experimental data. This Hamiltonian is called the Kondo model:

$$H = H_b + H_K \tag{A.10}$$

Where H_b is the term describing the conduction electrons expressed by a non-interacting electron gas and H_K describes the interaction between the electron gas and a localized magnetic moment modelled through the Heisenberg Hamiltonian.

$$H_b \;=\; \textstyle\sum_{\vec{k}\sigma}\varepsilon_{\vec{k}\sigma}c^\dagger_{\vec{k}\sigma}c_{\vec{k}\sigma}\;, and\;\; H_K = J\vec{S}\vec{s}_b \tag{A.11}$$

$\vec{S}$ represents the impurity spin and $\vec{s}_b$ is the spin of conduction electrons at the impurity site.

$$\vec{s}_b = \frac{1}{2}\frac{1}{N}\sum_{\vec{k}\vec{k}'}\sum_{\alpha\beta} c^{\dagger}_{\vec{k}\alpha}\vec{\sigma}_{\alpha\beta}c_{\vec{k}'\beta} \tag{A.12}$$

Here $\vec{\sigma}$ in $(A.12)$ are the Pauli matrices and not the spin as in $(A.11)$. The lattice has a finite size of N sites which are sent to infinity in the thermodynamic limit.

A.4 1-D Simple Impurity Anderson Model

To understand the local moment formation in systems with doped magnetic impurities, Anderson proposed a model to better understand this interaction [ref]. The simplest version comprises a single localized spin-degenerate level and a Coulomb repulsion when the level is filled with two electrons of opposite spin (numerical results for this setup are not considered in this thesis, rather only one electron). The local dynamics of this single-impurity Anderson model is then defined by the Hamiltonian:

$$H_{SIAM} = H_{imp} + H_b + H_{mix} \tag{A.13}$$

$$\hat{H}_{\mathrm{imp}} = \sum_{\sigma}\left(\epsilon_{d,\sigma} - \mu\right) d^{\dagger}_{\sigma}d_{\sigma} + U\, n_{d,\uparrow}n_{d,\downarrow}. \tag{A.14}$$

Where the operators $\hat{d}^{\dagger}$ and $\hat{d}$ create and annihilate electrons on the impurity level with spin components $\sigma = \pm 1$ and $n_{d,\sigma} = \hat{d}^{\dagger}\hat{d}$ is the particle number operator and μ is the chemical potential. Two electrons with different spin occupying the same impurity level cost a repulsive interaction energy $U > 0$ because of Coulomb Interaction, which is given by:

$$\epsilon_{d,\sigma} - \mu = -\frac{U}{2} + V_g + B\sigma\ . \tag{A.15}$$

This system is then coupled to a single conduction band which is modelled by a noninteracting electron gas:

$$H_b \quad = \quad \textstyle\sum_{\vec{k}\sigma}(\varepsilon_{\vec{k}} - \mu)\sigma)c^{\dagger}_{\vec{k}\sigma}c_{\vec{k}\sigma} \tag{A.16}$$

This impurity could be for example the d- or f-level of a transition metal atom embedded in a nonmagnetic metal. Anomoulous minimum in the electrical resistivity is observed at very low temperatures due to the interaction between the conduction electrons with the impurities [35] described by the Kondo model (A.11)

The interaction between the electron and the impurity bath due to hybridization is given by:

$$\hat{H}_{\text{hybridization}} = -V\sum_{\vec{k},\sigma}\left(d^{\dagger}_{\sigma}b_{\vec{k},\sigma,} + b^{\dagger}_{\vec{k},\sigma}d_{\sigma}\right) \tag{A.17}$$

Where V is the coupling strength between the electron and the impurity

Bibliography

[1] Jacob C Bridgeman and Christopher T Chubb. Hand-waving and interpretive dance: an introductory course on tensor networks. *Journal of Physics A: Mathematical and Theoretical*, 50(22):223001, May 2017.

[2] D. Suess, A. Eisfeld, and W. T. Strunz. Hierarchy of stochastic pure states for open quantum system dynamics. *Phys. Rev. Lett.*, 113:150403, Oct 2014.

[3] Xing Gao, Jiajun Ren, Alexander Eisfeld, and Zhigang Shuai. Non-markovian stochastic schrödinger equation: Matrix-product-state approach to the hierarchy of pure states. *Physical Review A*, 105(3), March 2022.

[4] Monique Combescure and Didier Robert. Fermionic coherent states. *Journal of Physics A: Mathematical and Theoretical*, 45(24):244005, may 2012.

[5] Wei-Min Zhang, Da Hsuan Feng, and Robert Gilmore. Coherent states: Theory and some applications. *Rev. Mod. Phys.*, 62:867–927, Oct 1990.

[6] M. Daoud and L. Gouba. Generalized grassmann variables for quantum kit (k-level) systems and barut–girardello coherent states for su(r + 1) algebras. *Journal of Mathematical Physics*, 58(5), May 2017.

[7] Atis Yosprakob. GrassmannTN: A Python package for Grassmann tensor network computations. *SciPost Phys. Codebases*, page 20, 2023.

[8] Zheng-Cheng Gu, Frank Verstraete, and Xiao-Gang Wen. Grassmann tensor network states and its renormalization for strongly correlated fermionic and bosonic states, 2010.

[9] Lajos Diósi and Walter T. Strunz. The non-markovian stochastic schrödinger equation for open systems. *Physics Letters A*, 235(6):569–573, November 1997.

[10] S. Flannigan, F. Damanet, and A. J. Daley. Many-body quantum state diffusion for non-markovian dynamics in strongly interacting systems. *Phys. Rev. Lett.*, 128:063601, Feb 2022.

[11] Ulrich Schollwöck. The density-matrix renormalization group in the age of matrix product states. *Annals of Physics*, 326(1):96–192, January 2011.

[12] F. Verstraete, V. Murg, and J.I. Cirac. Matrix product states, projected entangled pair states, and variational renormalization group methods for quantum spin systems. *Advances in Physics*, 57(2):143–224, March 2008.

[13] Jutho Haegeman, J. Ignacio Cirac, Tobias J. Osborne, Iztok Pižorn, Henri Verschelde, and Frank Verstraete. Time-dependent variational principle for quantum lattices. *Phys. Rev. Lett.*, 107:070601, Aug 2011.

[14] Johannes Motruk, Michael P. Zaletel, Roger S. K. Mong, and Frank Pollmann. Density matrix renormalization group on a cylinder in mixed real and momentum space. *Phys. Rev. B*, 93:155139, Apr 2016.

[15] Yosprakob, grassmanntn: A python package for grassmann tensor network computation. https://github.com/ayosprakob/grassmanntn, 2023.

[16] Ruofan Chen, Xiansong Xu, and Chu Guo. Grassmann time-evolving matrix product operators for quantum impurity models. *Physical Review B*, 109(4), January 2024.

[17] A. J. Leggett, S. Chakravarty, A. T. Dorsey, Matthew P. A. Fisher, Anupam Garg, and W. Zwerger. Dynamics of the dissipative two-state system. *Rev. Mod. Phys.*, 59:1–85, Jan 1987.

[18] Alexander Cyril Hewson. *The Kondo Problem to Heavy Fermions*. Cambridge Studies in Magnetism. Cambridge University Press, 1993.

[19] S. Diehl, A. Micheli, A. Kantian, B. Kraus, H. P. Büchler, and P. Zoller. Quantum states and phases in driven open quantum systems with cold atoms. *Nature Physics*, 4(11):878–883, September 2008.

[20] Frank Verstraete, Michael M. Wolf, and J. Ignacio Cirac. Quantum computation, quantum state engineering, and quantum phase transitions driven by dissipation, 2008.

[21] M. Blume, V. J. Emery, and A. Luther. Spin-boson systems: One-dimensional equivalents and the kondo problem. *Phys. Rev. Lett.*, 25:450–453, Aug 1970.

[22] Karyn Le Hur, Loïc Henriet, Loïc Herviou, Kirill Plekhanov, Alexandru Petrescu, Tal Goren, Marco Schiro, Christophe Mora, and Peter P. Orth. Driven dissipative dynamics and topology of quantum impurity systems. *Comptes Rendus. Physique*, 19(6):451–483, May 2018.

[23] P. Forn-Díaz, J. J. García-Ripoll, B. Peropadre, J.-L. Orgiazzi, M. A. Yurtalan, R. Belyansky, C. M. Wilson, and A. Lupascu. Ultrastrong coupling of a single artificial atom to an electromagnetic continuum in the nonperturbative regime. *Nature Physics*, 13(1):39–43, October 2016.

[24] Y. R. P. Sortais, H. Marion, C. Tuchendler, A. M. Lance, M. Lamare, P. Fournet, C. Armellin, R. Mercier, G. Messin, A. Browaeys, and P. Grangier. Diffraction-limited optics for single-atom manipulation. *Phys. Rev. A*, 75:013406, Jan 2007.

[25] A. Recati, P. O. Fedichev, W. Zwerger, J. von Delft, and P. Zoller. Atomic quantum dots coupled to a reservoir of a superfluid bose-einstein condensate. *Phys. Rev. Lett.*, 94:040404, Feb 2005.

[26] Karyn Le Hur, Loïc Henriet, Alexandru Petrescu, Kirill Plekhanov, Guillaume Roux, and Marco Schiró. Many-body quantum electrodynamics networks: Non-equilibrium condensed matter physics with light. *Comptes Rendus Physique*, 17(8):808–835, 2016. Polariton physics / Physique des polaritons.

[27] A. Furusaki and K. A. Matveev. Occupation of a resonant level coupled to a chiral luttinger liquid. *Phys. Rev. Lett.*, 88:226404, May 2002.

[28] T. Giamarchi. *Quantum Physics in One Dimension*. International Series of Monographs on Physics. Clarendon Press, 2004.

[29] T. Giamarchi and A. J. Millis. Conductivity of a luttinger liquid. *Phys. Rev. B*, 46:9325–9331, Oct 1992.

[30] Karyn Le Hur. Kondo resonance of a microwave photon. *Phys. Rev. B*, 85:140506, Apr 2012.

[31] Bennet Windt, Miguel Bello, Eugene Demler, and J. Ignacio Cirac. Fermionic matter-wave quantum optics with cold-atom impurity models. *Phys. Rev. A*, 109:023306, Feb 2024.

[32] A. González-Tudela and J. I. Cirac. Markovian and non-markovian dynamics of quantum emitters coupled to two-dimensional structured reservoirs. *Phys. Rev. A*, 96:043811, Oct 2017.

[33] J. S. Douglas, H. Habibian, C.-L. Hung, A. V. Gorshkov, H. J. Kimble, and D. E. Chang. Quantum many-body models with cold atoms coupled to photonic crystals. *Nature Photonics*, 9(5):326–331, April 2015.

[34] Xinyu Zhao, Wufu Shi, Lian-Ao Wu, and Ting Yu. Fermionic stochastic schrödinger equation and master equation: An open-system model. *Phys. Rev. A*, 86:032116, Sep 2012.

[35] W.J. de Haas, J. de Boer, and G.J. van dën Berg. The electrical resistance of gold, copper and lead at low temperatures. *Physica*, 1(7):1115–1124, 1934.